PRESSURE DROP MEASUREMENTS IN THE TRANSITION

REGION FOR A CIRCULAR TUBE WITH A

SQUARE-EDGED ENTRANCE

By

JODY R. AUGUSTINE

Bachelor of Science in Mechanical Engineering

The University of Southwestern Louisiana

Lafayette, Louisiana

1988

PRESSURE DROP MEASUREMENTS IN THE TRANSITION

REGION FOR A CIRCULAR TUBE WITH A

SQUARE-EDGED ENTRANCE

Thesis Approved:

A. J. Ghajar
Thesis Advisor

P. M. Moretti

_____

Norman N. Durham
Dean of the Graduate College

ii

ACKNOWLEDGMENTS

TABLE OF CONTENTS

LIST OF TABLES

LIST OF FIGURES

NOMENCLATURE

C_f fully developed skin friction coefficient

C_{fexp} fully developed skin friction coefficient obtained experimentally

C_{fl} fully developed skin friciton coefficient in the laminar flow regime

C_{ft} fully developed skin friction coefficient in the turbulent flow regime

C_{ftr} fully developed skin friciton coefficient in the transition flow regime

D_i inside diameter of the test section

f fully developed friction factor

f_{app} apparent friction factor

F turbine meter frequency and degree Fahrenheit

g gravitational acceleration

g_c gravitational constant

inwc   inches of water column

L test section length

nu   kinematic viscosity of test fluid

Re   Reynolds number, $Re = V_{avg}D_i/nu$

V_{avg} average velocity of test fluid

x local axial distance

ΔP differential pressure

ρ density of test fluid

τ_w wall shear stress

CHAPTER I

INTRODUCTION

An important design problem in industrial heat
exchangers arises when the flow inside the tubes falls in the
transition region between laminar and turbulent flow. The
Reynolds number where transition begins to occur, the
critical Reynolds number, for smooth round tubes can vary
from 2000 to 10000 in extreme cases. An enormous amount of
data and analytical modeling is available for fluid flow
processes in tubes in the laminar and fully-turbulent flow
regimes. However, very little has been done to investigate
the problems encountered in the transition flow regime. In
practical engineering design, the usual recommendation is to
avoid design and operation in this flow regime; however, this
is not always feasible under design constraints. It is the
purpose of this study to provide information about this flow
regime for use by both the engineering designer and the
academician.

This study was performed concurrently with a study of
heat transfer measurements in the transition region for a
circular tube with a square-edged entrance, Strickland
(1990). Future studies of the transition region will involve
pressure drop and heat transfer measurements with different
inlet configurations, pressure drop measurements under a

constant wall heat flux condition, intermittency measurements under constant wall heat flux and isothermal conditions, and flow visualization. This chapter discusses the reasons for research, the objectives, and the method of approach.

Reasons for Research

It should be noted that there are two common standards in the specification of friction coefficients used in the literature, the Fanning Friction Factor is denoted by "c_f" and the Moody Friction Factor is denoted by "f". In this study, when the term "skin friction coefficient" is used it is referring to the Fanning standard. The Moody standard is used only when referring to apparent friction factor, f_{app}. The discrepancy arises from the method in which the friction coefficients were derived. The two friction coefficients differ by a factor of four. For example, in the laminar flow regime $c_f = 16/Re$ and $f = 64/Re$. One must use caution when using friction coefficient correlations to realize which standard is being used.

The skin friction coefficient is defined in Equation (1.1) and the apparent friction factor is defined in Equation (1.2).

$$c_f = \frac{\Delta P \ D}{2 \ L \ \gamma \ V_{avg}^2} \qquad (1.1)$$

$$f_{app} = \frac{P_{o-x} \ D}{\frac{1}{2} \ x \ \gamma \ V_{avg}^2} \qquad (1.2)$$

In Equation (1.2) the term "ΔP_{o-x}" refers to the pressure drop from the inlet to a specific point down the tube.

In order to successfully predict pumping power requirements in industrial applications of viscous flows through smooth round tubes skin friction coefficient correlations are required. There are several skin friction coefficient correlations available. Table I states the presently available skin friction coefficient correlations for the laminar, transition, and turbulent flow regimes, Bhatti and Shah (1987). The correlations in Table I are denoted by "f" but utilize the Fanning standard.

The skin friction coefficient correlation for fully developed laminar flow is obtained through elementary fluid dynamics theory and has long since been known, $c_f = 16/Re$.

The correlation proposed by Shah (1977) for the apparent friction factor, f_{app}, for laminar flow is applicable only for a smooth circular duct with a short bell-mouthed entrance. The apparent friction factor, f_{app}, is defined as a friction coefficient which takes into account pressure drop in a tube caused by friction between the fluid and the tube wall and also pressure drop caused by the momentum flux in the development of the velocity profile. There are presently no available correlations for apparent friction factors in the transition and turbulent regions.

There are presently three available correlations for predicting fully developed skin friction coefficients in the transition region developed by Bhatti & Shah (1987),

TABLE I

FRICTION FACTOR CORRELATIONS FOR A SMOOTH CIRCULAR DUCT

INVESTIGATOR	CORRELATION	RECOMMENDED Re RANGE
Shah	$f_{app} = \dfrac{1}{Re} \left[\dfrac{3.44}{\zeta^{1/2}} + \dfrac{0.31/\zeta + 16 - 3.44/\zeta^{1/2}}{1 + 0.00021/\zeta^2} \right]$ where $\zeta = (x/D)/Re$ f_{app} = apparent friction factor	Laminar
Churchill	$\dfrac{2}{f} = \left\{ \dfrac{1}{[(8/Re)^{10} + (Re/36,500)^{20}]^{1/2}} + \left[2.21 \ln\left(\dfrac{Re}{7}\right) \right]^{10} \right\}^{1/5}$	Laminar, Transition and Turbulent
Hrycak & Andruskriw	$f = -3.10 \times 10^{-3} + 7.125 \times 10^{-6} Re - 9.70 \times 10^{-10} Re^2$	2,100 to 4,500
Bhatti & Shah	$f = A + \dfrac{B}{Re^{1/m}}$ where $A = 0.0054$, $B = 2.3 \times 10^{-8}$, $m = -\dfrac{2}{3}$ for $2,300 \le Re \le 4,000$ and $A = 1.28 \times 10^{-3}$, $B = 0.1143$, $m = 3.2154$ for $4,000 \le Re \le 10^7$.	2,300 to 10^7
Blasius	$f = 0.0791 \, Re^{-0.25}$	4×10^3 to 10^5
McAdams	$f = 0.046 \, Re^{-0.2}$	3×10^4 to 10^6
Bhatti & Shah	$f = 0.0366 \, Re^{-0.1818}$	4×10^4 to 10^7
Nikuradse	$f = 0.0008 + 0.0553 \, Re^{-0.237}$	10^5 to 10^7

4

TABLE I (Continued)

INVESTIGATOR	CORRELATION	RECOMMENDED Re RANGE
Drew et al.	$f = 0.0014 + 0.125 \, Re^{-0.32}$	4×10^3 to 5×10^6
Bhatti & Shah	$f = 0.00128 + 0.1143 \, Re^{-0.311}$	4×10^3 to 10^7
Prandtl Karman Nikuradse	$\dfrac{1}{\sqrt{f}} = 1.7372 \ln(Re\sqrt{f}) - 0.3946$	4×10^3 to 10^7
Colebrook	$\dfrac{1}{\sqrt{f}} = 1.5635 \ln\left(\dfrac{Re}{7}\right)$	4×10^3 to 10^7
Filonenko	$\dfrac{1}{\sqrt{f}} = 1.58 \ln Re - 3.28$	10^4 to 10^7
Techo et al.	$\dfrac{1}{\sqrt{f}} = 1.7372 \ln \dfrac{Re}{1.964 \ln Re - 3.8215}$	10^4 to 10^7

Churchill (1977), and Hrycak & Andruskiw (1974). The
correlations are listed in Table I. Churchill's correlation
is valid for all three fully developed flow regimes but the
Reynolds number ranges for Bhatti & Shah's and Hrycak &
Andruskiw's correlations are 2300 to 4000 and 2100 to 4500,
respectively. However, these correlations are based on data
obtained from making pressure drop measurements on a smooth
round tube with a rounded entrance. This study will provide
information and correlations associated with this flow regime
in a circular tube with a square-edged entrance.

For Reynolds numbers between 4000 and 100000 the well
established Blasius turbulent skin friction coefficient
correlation is available. For a smooth round tube with
square-edged entrance the lower limit for this correlation is
not well defined.

Table I also presents the other available skin friction
coefficients for fully developed turbulent flow. Some of
their Reynolds number ranges touch on the range used in this
study but they are generally used for turbulent flows with
higher Reynolds numbers.

Many heat transfer correlations for round tubes involve
the use of a skin friction coefficient. The data provided by
this study will aid in the development of heat transfer
correlations for smooth round tubes with a square-edged
entrance.

With the advent of hot-film anemometry the concept of
intermittency has been introduced into the field of fluid

dynamics research. Intermittency is defined as a degree of turbulence with the intermittency factor being zero for a fully laminar flow and one for a fully turbulent flow. The work of Ogawa and Kawamura (1987) presents skin friction coefficient and heat transfer correlations for transition flows with several inlet configurations involving the intermittency factor. The data from this study will aid in developing similar correlations.

Objectives

The objectives for this study are as follows:

1. to construct a versatile experimental setup to make pressure drop measurements with different inlet configurations, under a constant wall heat flux condition, and to provide the ability to make intermittency measurements in the test section.

2. to define the range of Reynolds numbers where the transition region occurs for a smooth round tube with a square-edged entrance thereby determining at what Reynolds numbers the fully developed laminar skin friction coefficient correlation is no longer valid and the Blasius fully developed turbulent skin friction coefficient correlation becomes valid.

3. to provide a correlation to predict fully developed skin friction coefficients in the transition region for this particular entrance and compare with those

developed for rounded entrances.

4. to compare the experimentally obtained skin friction coefficients with those listed in Table I for the fully developed laminar and turbulent flow regimes.

5. To determine what influences the square-edged entrance configuration has on the established laminar apparent friction factor correlation.

6. to develop guidelines for the development of the laminar and turbulent skin friction coefficients in the entrance region of a smooth round tube with a square-edged entrance.

7. to provide valuable data to later develop heat transfer correlations using skin friction coefficients.

8. to provide data to later develop skin friction coefficient correlations involving the concept of intermittency.

Method of Approach

The current work focuses on the study of fully developed skin friction coefficients in the transition flow regime and establishing the Reynolds number limits for this regime in a smooth round tube with a square-edged entrance. The well established laminar and fully turbulent flow regimes will also be studied to determine what effects this particular entrance configuration has on these flow regimes and relate

those observations to those made for the transition flow regime.

To make these observations pressure drop measurements will be made on a horizontal circular tube with a length to diameter ratio of 386. Although air is much easier fluid with which to perform this task, liquids will be used. A study of heat transfer in the same flow regime with the same entrance configuration will be performed concurrently with this study. By using liquids a greater range of Prandtl numbers can be achieved which will provide better data for developing heat transfer correlations. Therefore it is important to use liquids for the pressure drop measurements so the data can be used with greater confidence to make comparisons with the heat transfer data and so that heat transfer correlations involving skin friction coefficients can be developed more readily. The fluids to be used will be distilled water, ethylene glycol, and solutions of distilled water and ethylene glycol. The three types of fluids are necessary to provide a greater range of Reynolds numbers due to their range of viscosities.

The horizontal circular tube will be equipped with twenty-one pressure taps. The spacing and orientation of the pressure taps is displayed in Figure 2.2. The number of pressure taps was well thought out so as to provide as much information in the entrance region as possible without putting an excessive number of holes in the tube to distract from the characteristics of a smooth tube. Each of the

pressure tap holes was to be deburred with a special tool, described in Chapter II, to further ensure the characteristics of a smooth tube.

Preliminary calculations predicted the majority of the pressure drops for the experimental setup in the Reynolds number ranges required for the three types of fluid used to be between zero and fifty inches of water. The pressure drop between the closest spaced pressure taps was estimated to be as low as 0.1 inwc. There are presently no accurate differential pressure transducers that digitally measure differential pressures of liquids in this range. It was decided to use three analog differential pressure gauges, with increasing ranges, and a mercury manometer to make the necessary pressure drop measurements.

Upon studying the work of Shapiro and Smith (1957) a pressure gauge manifold was to be constructed. This manifold would allow pressure drop measurements to be made from the reference pressure tap to any of the other twenty pressure taps.

In order to reduce the pressure drop measurements to skin friction coefficients the thermophysical properties of the fluid had to be accurately determined. The work of Bohn, et al. (1984) presents equations for the thermal conductivity, density, viscosity, and Prandtl numbers of ethylene glycol-water mixtures for any concentration on a mass basis. These equations, listed in Appendix E, were incorporated into a computer program to calculate all of the

pertinent thermophysical properties of a given concentration of fluid for a given bulk temperature at given volume flow rate. This computer program , "ETH", and a comparison of its computed values with other sources is listed in Appendices D and E, respectively.

CHAPTER II

EXPERIMENTAL APPARATUS

Pressure drop measurements in the transition flow regime were studied in a horizontal circular tube with a square-edged entrance. The pressure drop study was part of a larger study that encompassed pressure drop and forced and mixed convective heat transfer measurements under a constant wall heat flux condition in the same flow regime with different inlet configurations. The experimental setup is shown in Figure 2.1. A versatile setup was required so that the effects of different inlet configurations and the effects of a uniform wall heat flux condition on pressure drop could be later studied. Distilled water, ethylene glycol, and ethylene glycol-water solutions were used as test fluids. The experimental setup, calibration procedure, experimental procedure, and method of data reduction are described as follows.

Description of the Equipment

Test Section

The test section was a seamless 316 stainless steel circular tube with an average inside diameter of 0.621 ± 0.002 inches (15.8 mm ± 0.013 mm) and outside diameter of
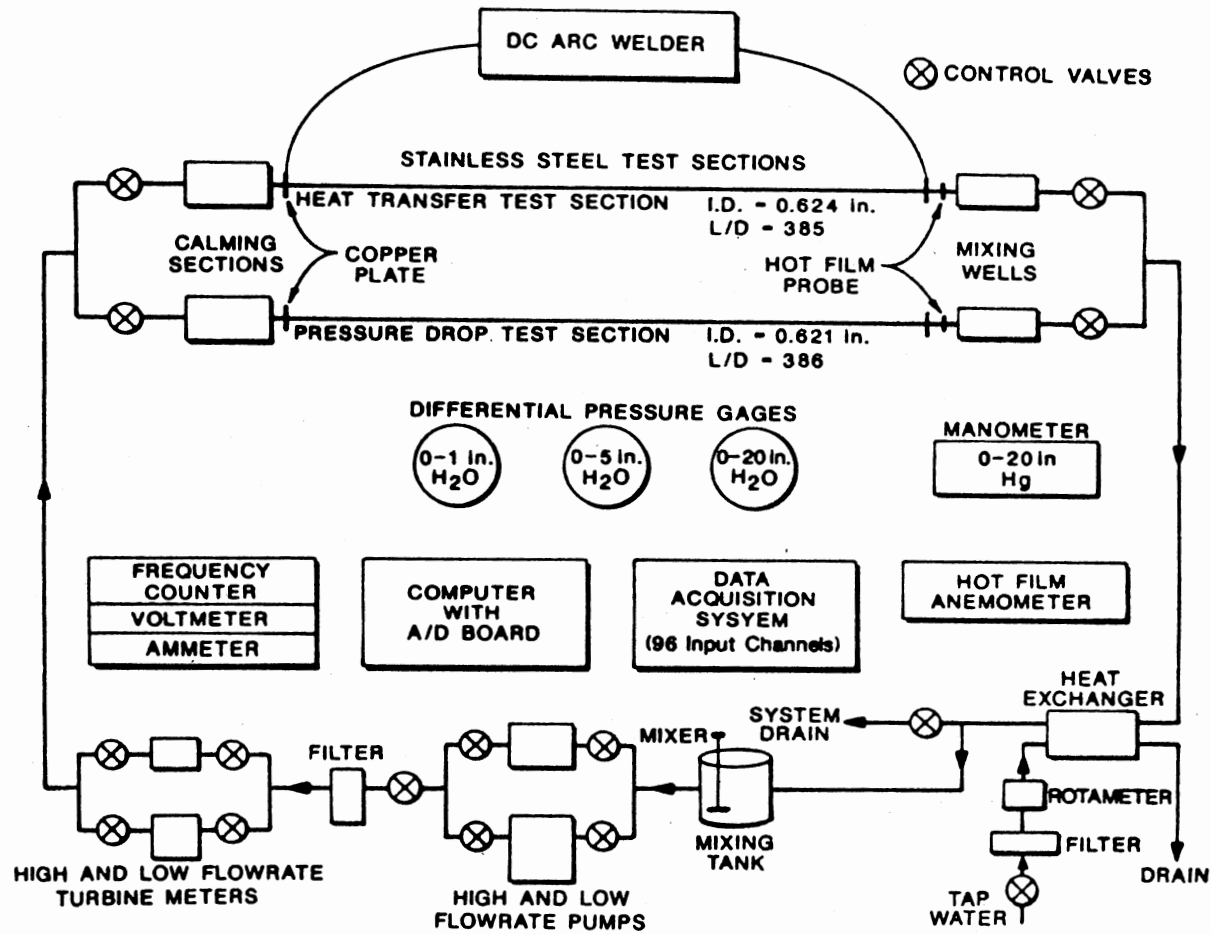
Figure 2.1 Schematic of the Experimental Setup

0.752 ± 0.001 inches (19.1 mm ± 0.007 mm). The total length
of the test section was 230.75 inches (5.861 m) providing a
length to diameter ratio (L/D) of 386. The test section was
purchased from the Precision Tubing and Fitting Co. of Tulsa,
Oklahoma. The test section was wrapped with fiberglass pipe
insulation and vapor seal. The total thickness of these
materials was approximately one inch. The test section was
leveled with the use of a surveying transit and wooden
spacers. The leveling of the test section was checked once
a week throughout the study.

Although not used in this study, at the end of the test
section a rectangular aluminum housing for the hot film probe
was heat expanded, positioned, and cooled to a water-tight
fit over the test section. The housing was 2.5" x 2.25" x
1.5" and had an additional hole machined to allow for the
insertion of the probe. A slot through the test section also
had to be machined to allow for the insertion of the probe.
The probe housing and the slot were machined by personnel at
the Mechanical Engineering North Labs at Oklahoma State
University.

Equipment for Generating a Constant Wall Heat Flux Condition

Although not used in this study, copper plates were
silver soldered near the inlet and exit of the test section,
as shown in Figure 2.2, for the purpose of attaching welding
cables to subject the test section to a constant wall heat
flux. The inlet plate was 1/4" x 10" x 10" and the exit

plate was 1/4" x 5" x 5". Supporting copper material and bus bars were bolted to the plates were sized to conform to the space limitations of the apparatus.

The heat flux source is a Lincoln Idealarc DC-600 three phase rectified type electric welder and will be used with variable voltage to produce a DC electric current through the test section. The welder has maximum power output of 26.4 KW.

To ensure minimal room heating and vibration effects from the welder it was located near an external wall where cooling air could be brought in from outside the room and exhausted outside the room through custom made plenums. Much of the exhaust noise will be alleviated in this manner. In order to prevent the welder from transmitting vibrations through the room, a 37" x 41" x 57" plywood box was placed over the welder. The sides of the box were lined with two inches of duct insulation. Ten refrigerator type damping pads were placed on the bottom of the welder to prevent the transmission of vibration through the floor.

Pressure Taps

Twenty-one holes of 5/64" (1.98 mm) diameter were drilled in the test section to accommodate twenty-one pressure taps. When drilling for the pressure taps, one has to ensure that the ratio of the tube wall thickness to tap hole diameter, t/D, is greater than 1.0 for minimum error, Benedict (1984). The diameter of the holes that were
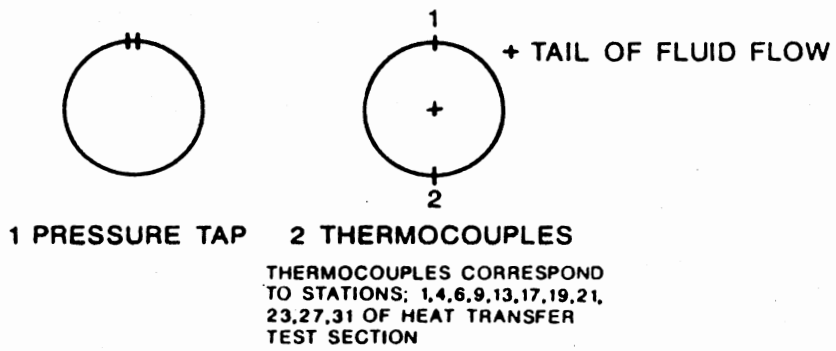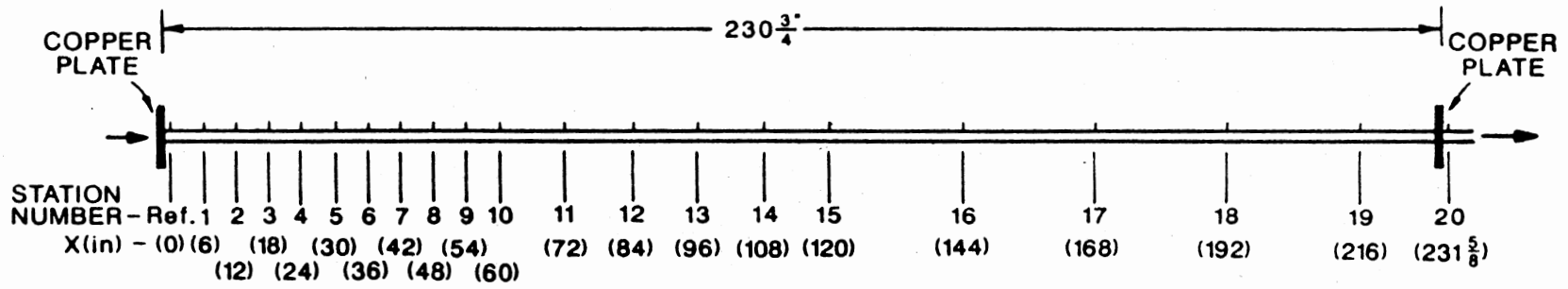
Figure 2.2   Schematic of the Test Section

drilled was 5/64" because that is the smallest size in which the deburring tool is available. The tap diameter used gave a t/D ratio of 0.82 which is close to 1.0 and is not belived to have induced any significant error. The hole spacing and pressure tap orientation is shown in Figure 2.2. After the holes were drilled they were followed with a deburring tool manufactured by Reynolds Tool Products (Anaheim, CA), Model # T-A BA 5/64. The holes had to be deburred in order to ensure the characteristics of a smooth tube, thus eliminating excess pressure drop and the onset of false transition flow. The pressure taps were standard saddle type self-tapping valves (1/2" - 1 1/2" capacity) with the tapping core removed. 1/4 inch I.D. vinyl tubing was used to connect the pressure taps to the pressure tap manifold.

Pressure Tap Manifold

A pressure tap manifold was constructed in order to make sequential pressure drop measurements down the test section (i.e. isolate different lengths of the test section in order to make pressure drop measurements from the reference pressure tap to the desired pressure tap). This apparatus is shown in Figure 2.3. The manifold consisted of five sections containing four valves each. The valves were PVC ball valves with 1/4" NPT threads on one end and a 1/4" - 3/8" hose barb on the other. They were purchased from the Industrial Plastics Corp. Each section was essentially a 1.5" x 1" x 8" aluminum block with a 0.125 inch hole drilled through the
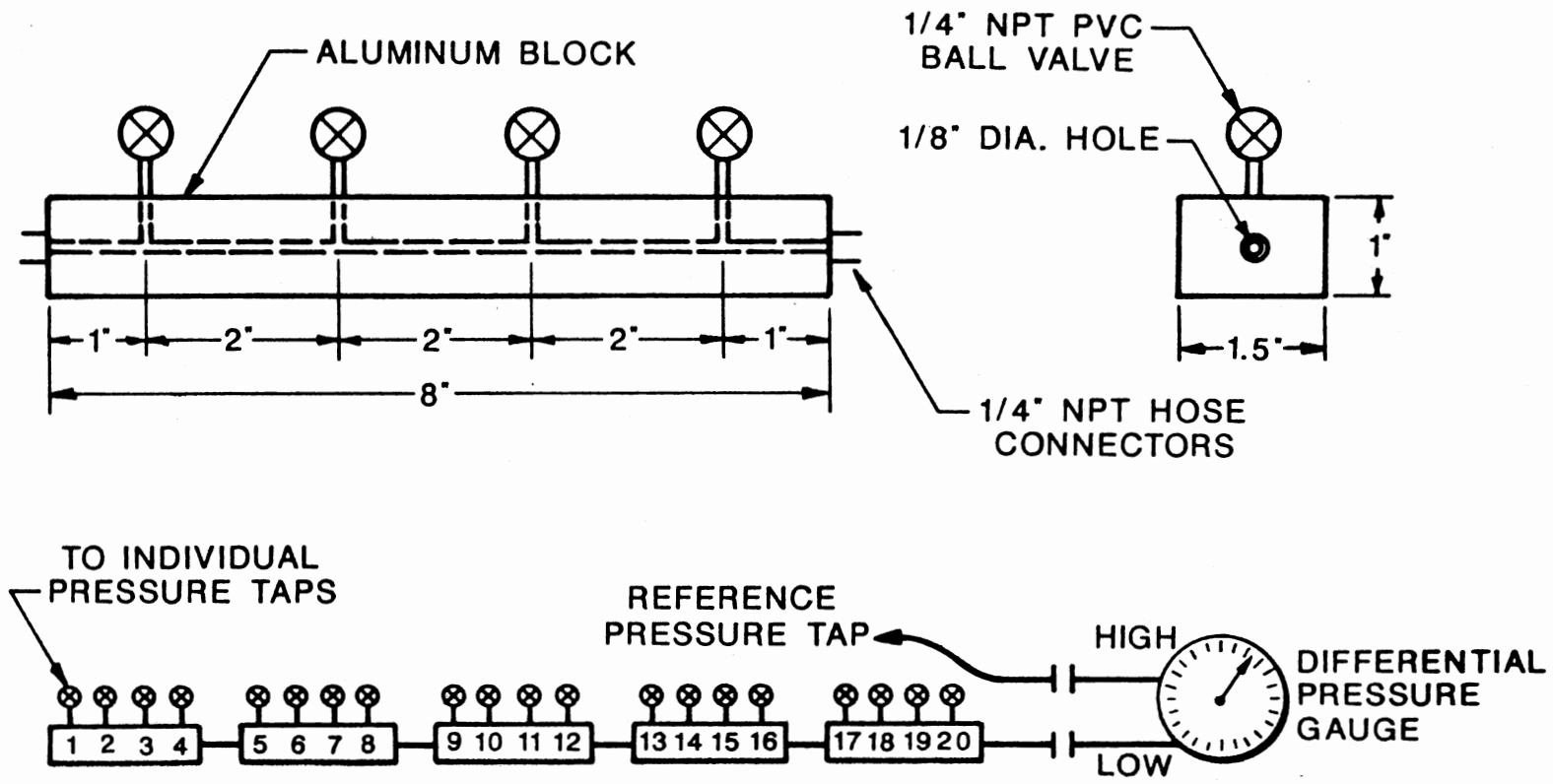
Figure 2.3 Schematic of the Pressure Tap Manifold

center. Four holes were drilled through the top and tapped
to accommodate the ball valves.

Calming and Inlet Sections

The calming and inlet sections, made from acrylic
plastic, were used to produce a uniform velocity distribution
in the test fluid before entering the test section. The
combination of the inlet section and the test section
produced a square-edged entrance configuration for the test
section. The calming and inlet sections and their dimensions
are shown in Figure 2.4. The flow entering the calming and
inlet sections encountered: 1) Three screens which were
machined from 1/2 inch acrylic plastic and contained 7/16"
diameter holes on a 0.6 inch equilateral triangular pitch; 2)
A 23 gauge galvanized steel mesh followed by tightly packed
soda straws and another 23 gauge mesh; and 3) An aluminum
insect screen mesh supported by 23 gauge galvanized steel
mesh. These components were encased by a 7 inch O.D.
plexiglass tube of 3/16 inch wall thickness. These
components were held in place by spacers constructed from 6
and 1/2 inch plexiglass tube of 3/16 inch wall thickness.
After the test fluid encountered these flow straighteners
it flowed undisturbed through the inlet section, 9.25 inches
of a 6 and 1/2 inch plexiglass tube. This was done to ensure
a uniform velocity distribution upon entering the test
section. The calming and inlet sections were also equipped
with air bleed valves which were used to evacuate air during
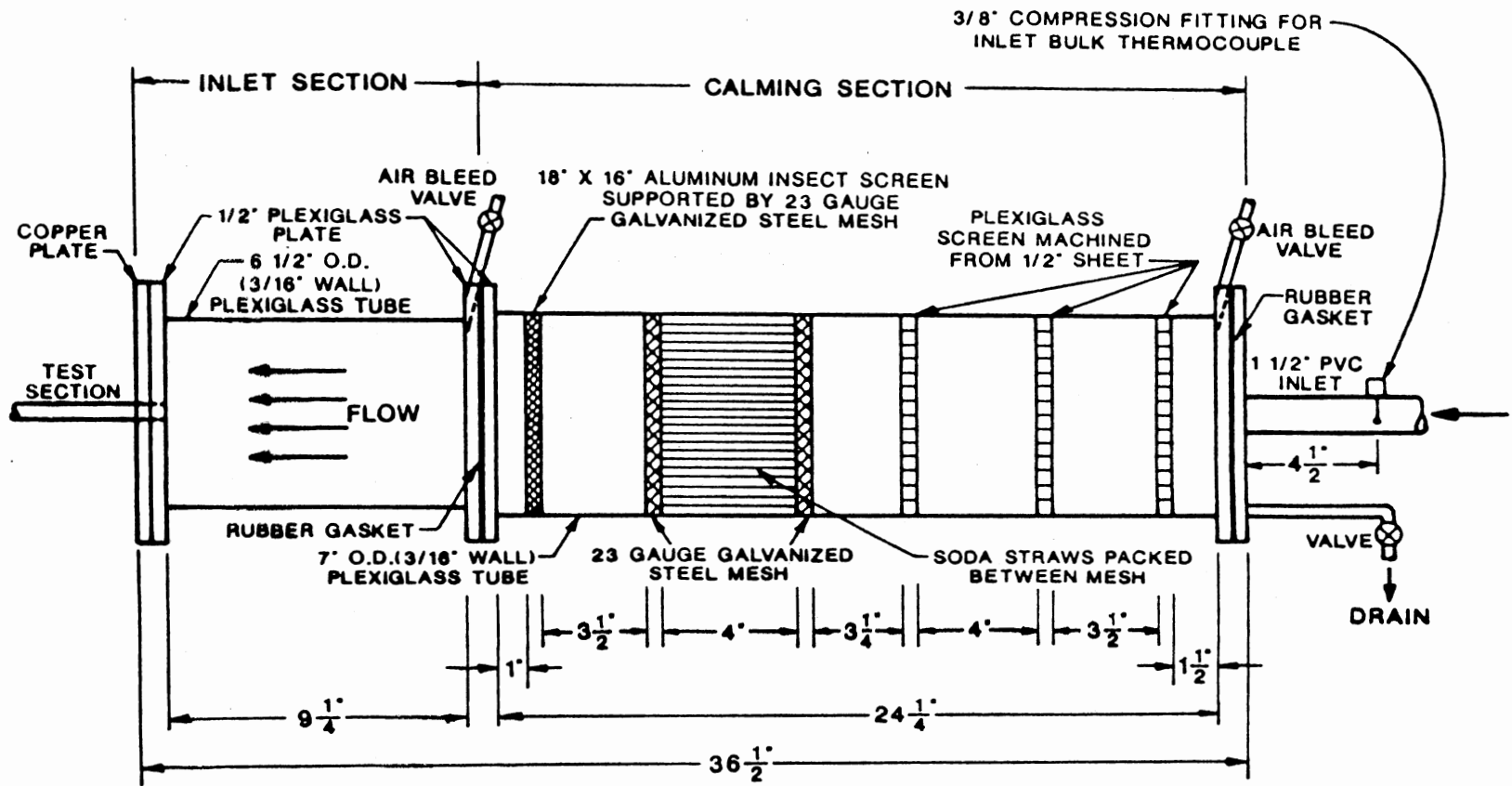
Figure 2.4   Schematic of the Calming and Inlet Sections

20

start up.

The inlet section had the versatility of easily being modified to incorporate a re-entrant, bell-shaped, or any other inlet configuration deemed feasible.

Mixing Well

To ensure a uniform fluid bulk temperature at the exit of the test section a mixing well was utilized. The mixing well was constructed from high temperature 1.25 inch schedule 40 CPVC pipe and is shown in Figure 2.5. Alternating acrylic baffles were placed in the well oriented from the top and from the bottom blocking 60% of the internal flow area. The baffles were held in place with a silicon sealant. These baffles caused the flow to be vigorously mixed thus ensuring a uniform bulk temperature at the exit of the mixing well. Near the end of the mixing well a T-type thermocouple (TT-T-30), permanently fixed inside a 1/4 inch aluminum tube approximately 2.5 inches long, was inserted into the flow area through a brass compression fitting. The mixing well is connected to the test section by an acrylic reducing adaptor cemented inside a 1.25 inch CPVC coupling.

Thermocouples

Although they were not used in this study, twenty-two thermocouples (Omega TT-T-30) were cemented with Omegabond 101 to the outside of the test section in the orientation shown on Figure 2.2. Omega EXPP-T-20 extension wire was used
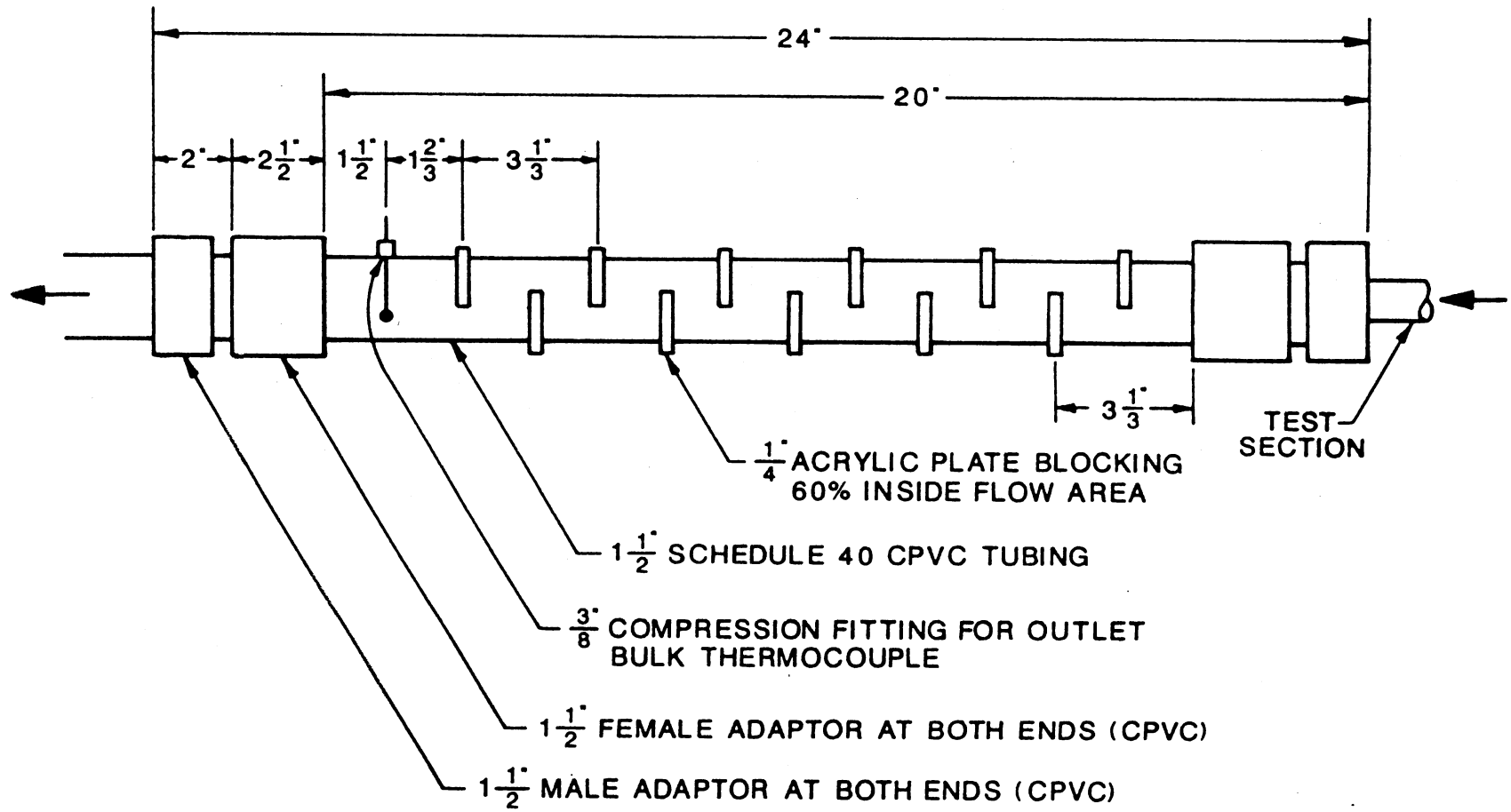
Figure 2.5 Schematic of the Mixing Well

for all the thermocouples. This was done to allow a more flexible experimental setup so that pressure drop measurements under a constant wall heat flux condition could be performed for a later study.

For this study one thermocouple was placed 4.5 inches before the entrance to the calming section in the 1.5 inch PVC pipe as shown in Figure 2.4. One thermocouple was also placed at the exit of the mixing well as shown in Figure 2.5. These thermocouples were mounted in the same manner as those used for the heat exchanger and were used to monitor the inlet and exit bulk temperatures of the test fluid. These thermocouples were monitored with ECD 5100 Forty Channel Data Logger manufactured by Electronic Controls Design.

Pumps

For low flow rates a pump manufactured by Little Giant Pump Co., model 4-MD, was used. It produced a maximum flow rate of 4.5 gpm at 3100 rpm using a 1/12 hp motor. For high flow rates a pump manufactured by Oberdorfer Pumps, model SKH35FN193T, was used. It produced a maximum flow rate of 11 gpm at 3450 rpm using a General Electric 1/3 hp motor.

To minimize the vibrations produced by the pumps during operation they were mounted inside a plywood box using rubber damping material approximately 3/8 inches thick. The box had dimensions of 57 inches-wide, 30-inches high, and 16-inches deep. The interior walls of the box were lined with one inch of duct insulation and the entire box was isolated from the

floor with twelve refrigerator type rubber dampers to suppress additional vibrations. In addition, rubber hoses were connected to the pump box at both the upstream and downstream ends to prevent vibration transmission to the fluid return tubing.

Turbine Meters

For low flow rates a Cox Flowmeters, model AN 8-6, 1/2 inch turbine meter was used over a frequency range of 140 to 1140 Hz accommodating flow rates from 0.5 to 6.0 gpm. For high flow rates a Halliburton 1 inch turbine meter was used over a frequency range of 50 to 150 Hz accommodating flow rates to 10.5 gpm. Both turbine meters had a linearity of +0.5% of reading and a repeatibility of less than +0.10% of reading.

The turbine meters were incorporated into an assembly using 1.5 inch PVC ball valves at both ends of each to ensure no fluid entrainment from the one which is inactive at any given time. The calibration procedures for the turbine meters are detailed in the calibration section of this chapter.

Frequency Counter

A Hewlett-Packard model 5314A universal counter was used to indicate the frequency of the turbine meters during operation. The input frequency range for the 5314A is 10 Hz to 100 MHz, with a sensitivity of 25 millivolts rms to 100

MHz, and 0.075 volts peak to peak at a minimum pulse of 5 nanoseconds. The resolution and accuracy are to the least significant digit, LSD.

During operation of the turbine meters at low frequency, frequency instability problems were observed. To solve this problem, a variable gain amplifier was constructed by an Instruments Technician in the Mechanical & Aerospace Engineering Instruments Shop. It had a gain from one to five to produce a stable signal at low frequencies.

Heat Exchanger

A 21.2-ft^2 (1.97-m^2), 1-2 shell and tube heat exchanger manufactured by the ITT Standard Company (Model BCF #04036) was used to keep the test fluid at a constant temperature. The heat exchanger had a maximum duty of 67190 Btu/hr (19.7 KW). It was purchased from the Thermal Engineering Co. of Tulsa, Oklahoma. The cooling fluid was utility water and its line was equipped with an Omega FL-9028 rotameter with a flow rate range of 4 to 28 gpm, an accuracy of ±5% full scale, and a repeatability of ±1% full scale. The cooling water line was also equipped with a Teel Water Systems model 2P227 double cartridge filter to remove impurities and avoid fouling in the heat exchanger. A 1.25 inch schedule 40 PVC pipe carried the cooling water to the exchanger and away from the exchanger to the waste water trough. Four TT-T-30 thermocouples, mounted inside 1/4 inch aluminum tubes approximately two inches long with silicon sealant, were

inserted through brass compression fittings. These
assemblies were mounted in the PVC pipes near the heat
exchanger to monitor the four stream temperatures with the
ECD 5100 Data Logger.

Differential Pressure Gauges and Manometer

To measure the small differential pressures created by
the transition flow of a liquid, three differential pressure
gauges were used. The gauges were manufactured by the Dwyer
Instrument Corporation and were models Capsuhelic 4001-B,
4005-B, and 4020-B. Their ranges were 0-1 inwc, 0-5 inwc,
and 0-20 inwc, respectively. The postscript "B" refers to
the fact that optional brass cases had to be used because of
the water based test fluid.

For differential pressures greater than 20 inwc the
differential pressures could be accurately measured with a
mercury manometer. For this case a 20" U-tube mercury
manometer was used. It was manufactured by the Meriam
Instrument Corporation, model # 10AA25WM.

Quick disconnect fittings purchased from the Cole-Palmer
Corporation were used to connect each of the pressure gauges
and the manometer to the pressure tap manifold.

Reservoir

A 16 gallon cylindrical polyethylene tank, cover, and
mixer were purchased from the Industrial Plastics Corp. The
tank was sixteen inches in diameter and twenty-one inches in

height. The mixer, used to ensure a uniform temperature distribution in the tank, was equipped with a 1/40 hp 1550 rpm motor and mixing blade.

Test Fluids

Distilled water, 60% ethylene glycol (by mass), and 100% ethylene glycol solutions were used as test fluids. The ethylene glycol was purchased from the Delta Chemical Company. The distilled water was obtained from the Oklahoma State University Chemical Engineering Department.

Fluid Return Piping

Since the test fluid may be heated, there is a high temperature 1.5 inch schedule 40 CPVC pipe running from the mixing well to the heat exchanger. Exiting the heat exchanger, standard 1 inch schedule 40 PVC pipe and a 1 inch PVC ball valve allows for system drain or return to the reservoir. Exiting the reservoir, the test fluid goes through 1/2 inch schedule 40 PVC to the pump box. After the pump assembly a 1/2 inch stainless steel ball valve is used for flow control before the fluid enters a Teel Water Systems model 2P227 double cartridge filter system using two model 1P753A cartridges. Essential to protect the fragile hot film probe, the filter removes impurities as small as 5 microns. The fluid is then carried through 1.5 inch schedule 40 PVC to the turbine meter assembly and from the turbine meter assembly to the calming section. 1.5 inch schedule 40 PVC

ball valves were used to direct the flow to either of the two test sections or to the additional flow visualization test section.

Experimental Calibrations

ECD 5100 Data Logger

The model 5100 data logger required a calibration procedure outlined in the operation manual. To perform the calibration a precision DC voltage source was used. This voltage source manufactured by the Electronic Development Corporation, model MV116, had an accuracy of ± 1 microvolt. With the data logger held on channel number one, a 2.00000 volt voltage was applied to the channel. The variable resistors within the unit were adjusted until the display indicated exactly 2.0000 volts.

Thermocouples

The inlet and exit bulk temperature thermocouples were calibrated using an ice-bath technique. The thermocouples were placed in an insulated bath of ice water and were connected to the ECD 5100 Data Logger using the same extension wire used throughout the study. After allowing the thermocouples to come to a steady state the temperature reading from the data logger was recorded. The thermocouples were accurate within a maximum of ± 0.5 F in all cases over the range of temperatures encountered.

Differential Pressure Gauges

The 0-1 inwc differential pressure gauge was checked against a 0-1 inwc slant tube manometer (also manufactured by Dwyer). The two devices were placed in parallel and were subjected to an equal pressure provided by a compressed air jet. After making minor adjustments to the differential pressure gauge with the fine adjustment screw on the face of the gauge, the gauge and the manometer were in full agreement throughout the entire 0-1 inwc range. This calibration was checked three times during throughout the study. The fine adjustment screw was never adjusted except during calibration checks.

The 0-20 inwc gauge had a large enough range to allow it to be checked against the mercury manometer. To accomplish this the system had to be in operation in order to generate a pressure differential. Using the pressure conversion chart provided by Dwyer (converting inwc to in. Hg), several differential pressures in the 10 to 20 inwc range were noted of the gauge and compared to the manometer readings. The gauge was adjusted accordingly using the fine adjustment screw on the face of the gauge until the gauge and the manometer were in full agreement. This procedure was repeated once a week throughout the study.

Once the 0-1 inwc gauge and the 0-20 inwc gauge were adjusted properly they could be used to adjust the 0-5 inwc gauge. This was done by starting the system and running

through a series of pressure drops from 0 to 5 inwc and using

. all three gauges. The 0-5 inwc gauge was adjusted so that a

one inch reading on the 0-1 inwc gauge corresponded to a one

inch reading of the 0-5 inwc gauge. Similarly, the 0-5 inwc

gauge was also adjusted so that five inch reading on the 0-20

inwc gauge corresponded to five a inch reading on the 0-5

inwc gauge. This procedure was repeated once a week

throughout the study.

At no time were the differential pressure gauges out of

adjustment by more than their accuracy reported by the

manufacturer, ±3%.

Turbine Meters

The flow rate through the two turbine meters was

calibrated against the frequency of the impeller rotation.

The calibration required a stopwatch, frequency counter, and

at least two persons. A tweny-five inch ruler graduated to

1/16 inches was taped to the inside of the reservoir. The

pump was switched on and allowed to run for a few seconds

until normal operation occurred and to allow the test fluid

to reach a uniform flow. Noting the initial height and

frequency, the reservoir level was allowed to drop in height

at the instant the stopwatch was activated. The fluid passed

through the entire system and exited to a catch container.

At certain time increments during the fluid collection, the

frequency indicated by the counter was recorded. When

roughly three to five gallons of test fluid had drained from

the reservoir, or a reasonable period of time had elapsed for the considered flow rate, the stopwatch and fluid flow were simultaneously stopped. The final height of the fluid in the reservoir was recorded and average frequency over the time interval was calculated. Using the time interval, reservoir diameter, and change in reservoir height, the volume flow rate was calculated. This volume flow rate was then correlated with the calculated average frequency. The procedure was repeated at representative values over the available frequency range of both turbine meters (approximately fifteen points). Each of these representative values were repeated three times to obtain averages. This averaged data was then correlated using a linear least squares curve fit. The minimum correlation coefficient attained was 99.90%, the maximum was 99.99%. Figures 2.6 and 2.7 illustrate the data collected for both meters and curve fits (including correlation coefficients) for all fluid concentrations used.

A computer program called "GPMCALC" was written to enable quick determination of flow rate given frequency or vice versa. This program is applicable for both turbine meters and all the fluid concentrations used. The complete program is listed in Appendix D.

Calibration Runs

To compare the accuracy of the experimental setup to the established skin friction coefficient correlations for
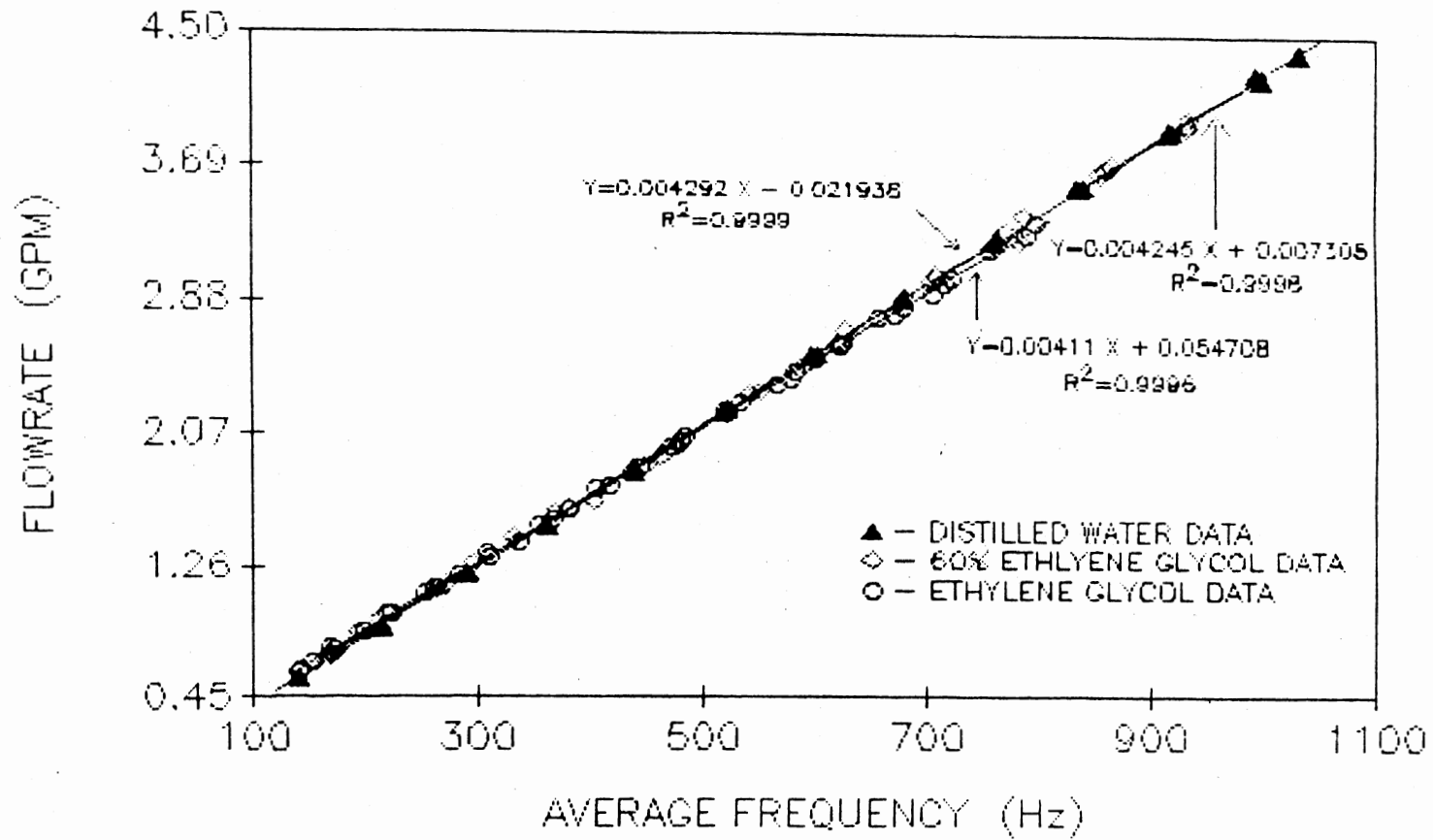
Figure 2.6   Calibration Data for the Small Turbine Meter
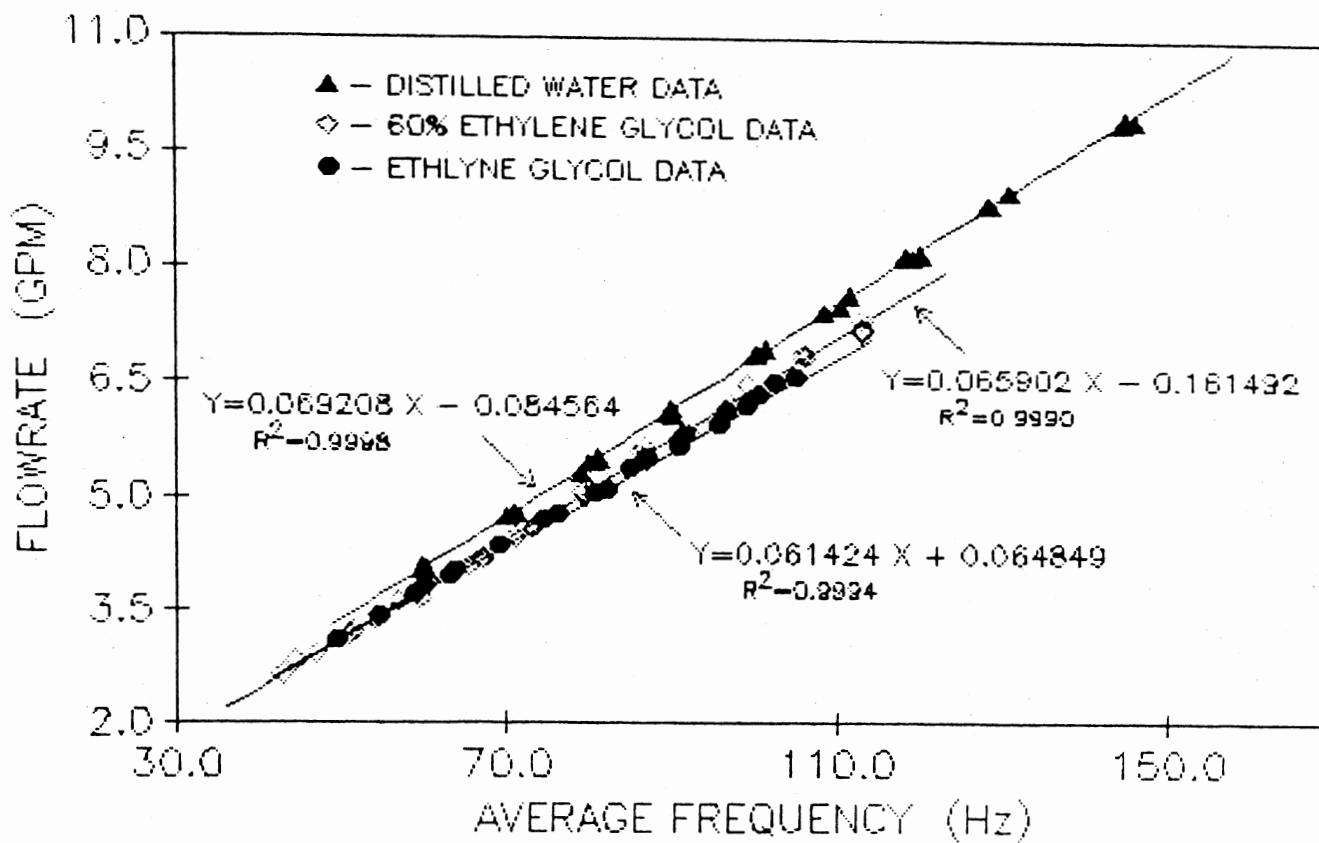
Figure 2.7   Calibration Data for the Large Turbine Meter

turbulent flow, distilled water was subjected to steady state fully turbulent flow with Reynolds numbers greater than 10000. Five fully developed skin friction coefficients were obtained for Reynolds numbers ranging from 11030 to 14970. The method used to obtain the fully developed skin friction coefficients was the same as that described in the section of this chapter on data reduction. When compared to the Blasius skin friction coefficient correlation for turbulent flow in round tubes, the experimental values obtained ranged from -2.1% to -4.6%. The values were assumed to be well within the accuracy of the Blasius correlation. From this point the system was considered to be behaving as expected and the data was considered valid. This calibration data is shown in Figure 2.8.

Start-Up and Operating Procedure

The following procedures were followed for each run:

1. All entrance and exit valves for the pressure drop test section were opened. All entrance and exit valves for the for the heat transfer test section were closed.

2. The entrance and exit valves for the desired turbine meter (high-flow or low-flow) were opened. The frequency counter and amplifier were turned on.

3. All valves on the pressure tap manifold were closed to avoid over pressurizing the differential pressure gauges.
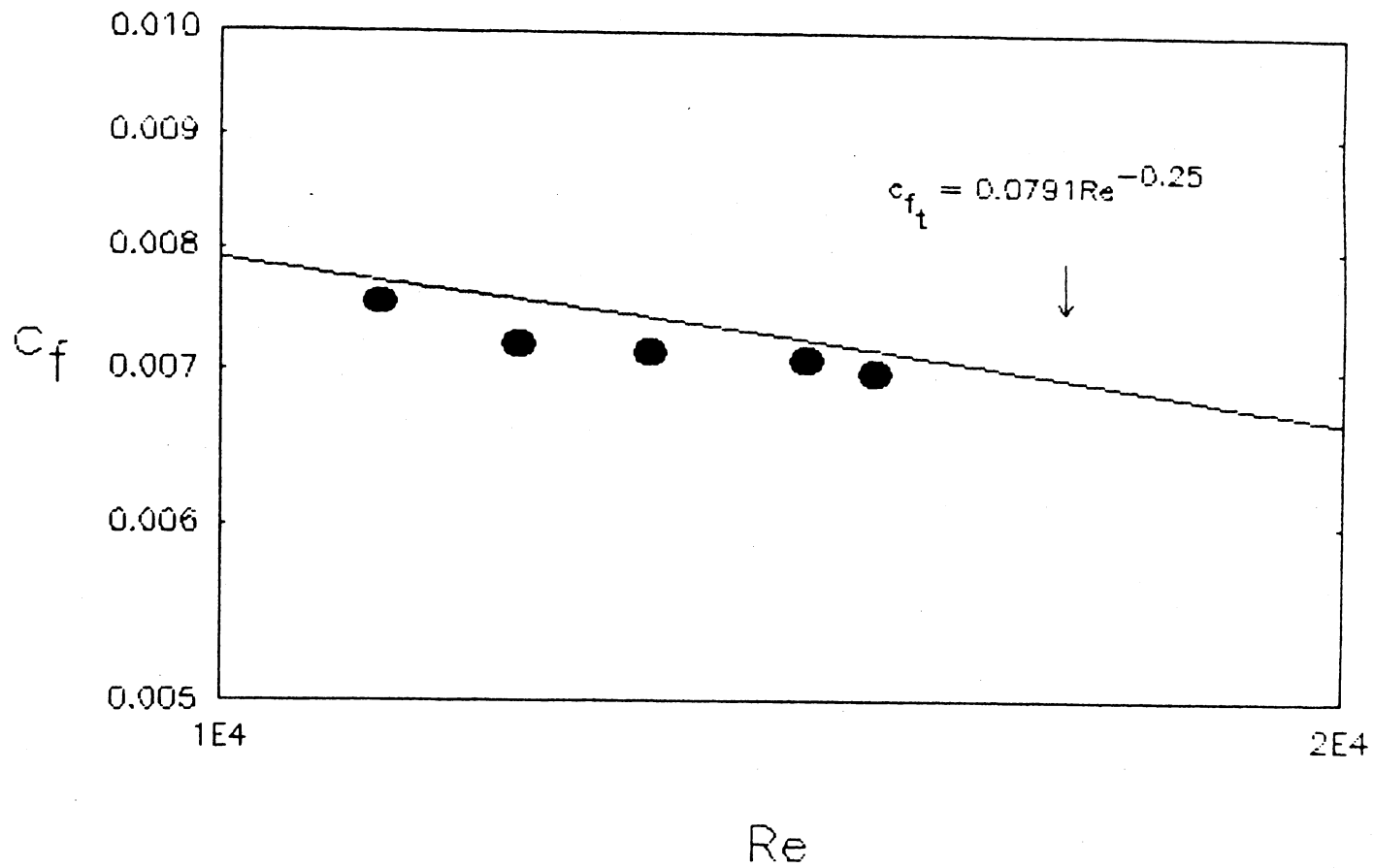
Figure 2.8 Calibration Data for the Test Section

$$c_{f_t} = 0.0791Re^{-0.25}$$

4. The entrance and exit valves for the desired pump
   (high-flow or low-flow) were opened and the pump
   turned on.

5. After checking for leaks on the entire test section,
   excess air was bled off of the calming and inlet
   sections.

6. The cooling water valve was opened (8 gpm) for the
   purpose of removing the heat added to the test
   fluid by the pump thereby allowing steady state
   conditions.

7. The ECD 5100 Data Logger was turned on to monitor
   the inlet and exit bulk temperatures of the test
   fluid. When the two temperatures were nearly
   equal (within 0.2 F of each other) and their
   temperatures did not change, the system was
   considered to be at steady state conditions.
   This usually required about two hours.

8. While steady state conditions were being achieved,
   the flow control valve was adjusted to reach the
   desired Reynolds number. The determination of the
   desired flow rate for a pre-selected Reynolds
   number was an iterative procedure. Once the test
   fluid temperature was relatively constant, that
   temperature was entered into the "ETH" computer
   program (Appendix D) as well as several different
   flow rates until the flow rate for the
   pre-selected Reynolds number was determined. This

flow rate was then entered into the turbine meter
calibration program "GPMCALC" (Appendix D), where
the desired turbine meter frequency was
determined. After steady state conditions were
achieved, meaning the data logger and frequency
counter readings were constant, the Reynolds
number was again checked with the computer
programs to see if it was still at the pre-
selected value. If the Reynolds number proved
unsatisfactory, the procedure was repeated.

9. The 0-20 inwc differential pressure gauge was then
connected (quick disconnect fittings were used for
each gauge as well as the manometer) to the
pressure tap manifold. Manifold valve No. 1 was
then opened to determine the differential pressure
from the reference pressure tap to pressure tap
No. 1. If the differential pressure was less than
five inches of water, the 0-5 inwc gauge was
connected. If the differential pressure reading
on the 0-5 inwc gauge was less than one inch of
water, the 0-1 inwc gauge was connected.

10. Once the needle on the gauge had reached its final
value, the reading was recorded. Manifold valve
No. 1 was then closed and manifold valve No. 2 was
opened. If the differential pressure measured at
pressure tap No. 2 was greater than the range of
the gauge used for pressure tap No. 1 then the

next higher range gauge (or manometer) was then
connected. Again, once the needle on the gauge
had reached its final value, the reading was
recorded. This procedure was repeated
successively with pressure taps Nos. 1 through 20.

11. Several runs were made to obtain averages for the
differential pressures at each station (1 through
20). This procedure is explained further in the
section of this chapter on data reduction.

12. The pump was shut off.

13. The data logger was turned off.

14. The entrance and exit valves to the pressure drop
test section were closed.

Some of the Problems Encountered

The quick-disconnect fitting that were used to connect
the differential pressure gauges and manometer to the
pressure tap manifold caused air bubbles to appear in the
lines after repeated connecting and disconnecting. This
problem was solved by using air bleed valves on the
differential pressure gauges. Whenever air bubbles would
appear the bleed valves were opened until the bubbles were
out of the lines. When air bubbles appeared in the manometer
lines, the lines had to be removed from the manometer and
re-filled with test fluid.

As the flow rate was decreased in order to attain lower
Reynolds numbers, the response time of the differential

pressure gauges grew increasingly longer. This was caused by the lack of system pressure on the gauges themselves. At flow rates near 1.5 gallons per minute, the response time of the gauges was approximately ten minutes. At flow rates below 1.5 gallons per minute the response time was great enough to render pressure drop measurements in this range unfeasible. No problems were encountered with the response time of the mercury manometer.

Data Reduction

In order to calculate the Reynolds number and skin friction coefficients for different flow rates a computer program was developed to calculate the thermophysical properties of ethylene glycol-water solutions. The computer program, "ETH", utilizes the correlations developed by Bohn, et.al.(1984) for density, absolute viscosity, thermal conductivity, and Prandtl number of ethylene glycol-water solutions. From these properties the program also calculates secondary properties, properties that are calculated from the properties that have correlations, such as coefficient of thermal expansion, kinematic viscosity, specific heat, and thermal diffusivity. The program prompts the user for the mass concentration of ethylene glycol (0 for pure water and 1 for pure ethylene glycol), volume flow rate, average bulk temperature, wall temperature, and tube diameter. From this information the program calculates the thermophysical properties as well as an average fluid velocity, Reynolds

number, and Grashof number. A listing of the "ETH" computer
program is given in Appendix D. A listing of the
correlations and a comparison of the calculated
thermophysical properties with other sources is given in
Appendix E.

An extension of the "ETH" computer program was developed
to calculate apparent friction factors from the measured
differential pressures. This program was called "FFC",
Friction Factor Calculations, and is listed in Appendix D.
Once the "ETH" program had been executed, the values for
Reynolds number, average fluid velocity, and density were
sent to "FFC". The x/D ratios for each pressure tap location
are stored in the program. Therefore, the only inputs in the
"FFC" program were the last pressure tap station read in
inches of water and the average differential pressure (either
in. of water or in. of Hg) between the reference pressure tap
and each pressure tap location. The apparent friction
factors were then calculated with Equation (1.2).
For the purpose of calculating apparent friction factors the
term "L" refers to the tube length between the reference
pressure tap and the pressure tap station over which the
differential pressure was measured.

In order to calculate the apparent friction factors and
the fully developed skin friction coefficients the following
procedure was used. Once a steady state was achieved the
pressure drops for stations 1 through 18 and station 20
(station 19 was used as a vent) were recorded and the

procedure was repeated three additional times. The four pressure drops for each station were then averaged. These nineteen average pressure drops were then reduced to apparent friction factors using the "FFC" computer program

The procedure for reducing the data to fully developed skin friction coefficients is as follows. The average pressure drop from the reference pressure tap to station 14 was subtracted form the average pressure drop from the reference pressure tap to station 20. The procedure was repeated for stations 15, 16, 17, and 18. The pressure tap stations 1 through 13 were not used for the fully developed skin friction coefficient calculations so as to avoid any possible entrance effects. These fully developed pressure drops and their respective tube lengths as well as the density and average velocity of the test fluid were entered into Equation (2.1). From this information, five fully developed skin friction coefficients were calculated for a given Reynolds number. Of these five fully developed skin friction coefficients, the highest and lowest values were discarded and the remaining three were averaged. This average value was taken as the fully developed friction factor for the given Reynolds number. The same procedure was used for the laminar, transition, and turbulent flow regimes. The reader is referred to Appendix B for a sample calculation illustrating this procedure.

CHAPTER III

RESULTS AND DISCUSSION

In order to study fully developed skin friction
coefficients in the transition flow regime, apparent and
fully developed friction factors in the well established
laminar and turbulent flow regimes were experimentally
obtained. The spectrum of Reynolds numbers covered
throughout the study ranged from 512 to 14970. By covering a
large range of Reynolds numbers the validity of the
experimental setup could be verified with the established
correlations and entrance effects in the established flow
regimes could aid in predicting the behavior of the
transition flow regime. A listing of the Reynolds numbers
covered, their respective fully developed skin friction
coefficients and the test fluid concentration used in
obtaining them is included as Table II. The source for all
of the data obtained in the study is listed in Appendix A.

Moody Diagram

The data, listed in Table II, is plotted as a Moody
diagram in Figure 3.1. The method for obtaining these fully
developed skin friction coefficients is described in Chapter
II. From the Moody diagram it can be seen that the data

42

TABLE II

FULLY DEVELOPED SKIN FRICTION COEFFICIENTS AND THE FLUID CONCENTRATIONS USED TO OBTAIN THEM

100% Ethylene Glycol

Re	C_f
512	0.0320
979	0.0165
1520	0.0104
1685	0.00930
1860	0.00838

60% Ethylene Glycol

Re	C_f	Re	C_f
2055	0.00740	2610	0.0104
2090	0.00745	2710	0.0106
2120	0.00815	2800	0.01075
2150	0.00856	2980	0.0108
2195	0.00888	3140	0.01075
2310	0.00940	3460	0.0107
2390	0.00949	3690	0.0105
2450	0.00980	4400	0.00973
2510	0.0101	4620	0.00955

100% Distilled Water

Re	C_f	Re	C_f
5080	0.00913	11030	0.00753
5970	0.00927	12020	0.00720
6990	0.00858	13030	0.00713
8980	0.00808	14350	0.00708
10000	0.00785	14970	0.00698

---

follows the laminar skin friction coefficient line closely until Reynolds numbers of slightly greater than 2000. At this point the onset of transition is seen to occur. The fully developed skin friction coefficients begin to increase in a parabolic manner until they reach the turbulent skin friction coefficient line. At Reynolds numbers greater than 3000 the data begins to closely follow the turbulent skin friction coefficient line. A plot of the percent deviation of the experimental data from the fully developed laminar skin friction coefficient correlation in the laminar region (512 < Re < 1980) is included as Figure 3.2. The percent deviation in the laminar region ranged from 2.1% to -2.7% which was considered to be well within the tolerance of the system. The uncertainty analysis performed for the data obtained in this study is shown in Appendix C and shows the maximum probable error in the data to be +5.23%. A plot of the percent deviation of the experimental data from the Blasius fully developed skin friction coefficient correlation in the turbulent region (2980 < Re < 14970) is included as Figure 3.3. The percent deviation in the turbulent region ranged from 3.5% to -5.0% which is within the accuracy of the experimental data.

Table I, listed in Chapter I, lists other turbulent flow friction factor correlations by Bhatti & Shah and Drew et al. but in the range of turbulent Reynolds numbers used in this study these correlations differed from the Blasius correlation by less than 1%. It is for this reason that the
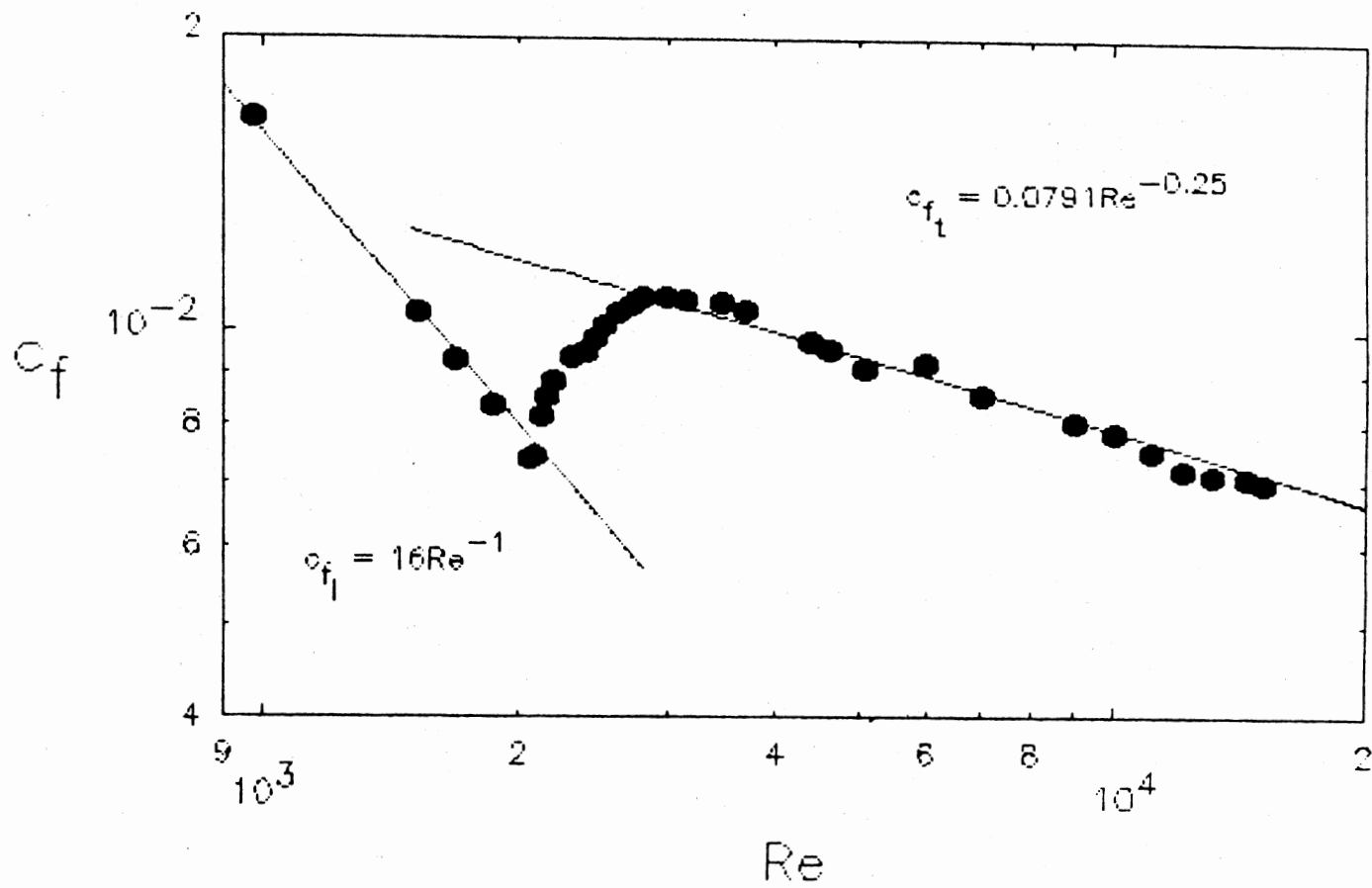
Figure 3.1 Moody Diagram
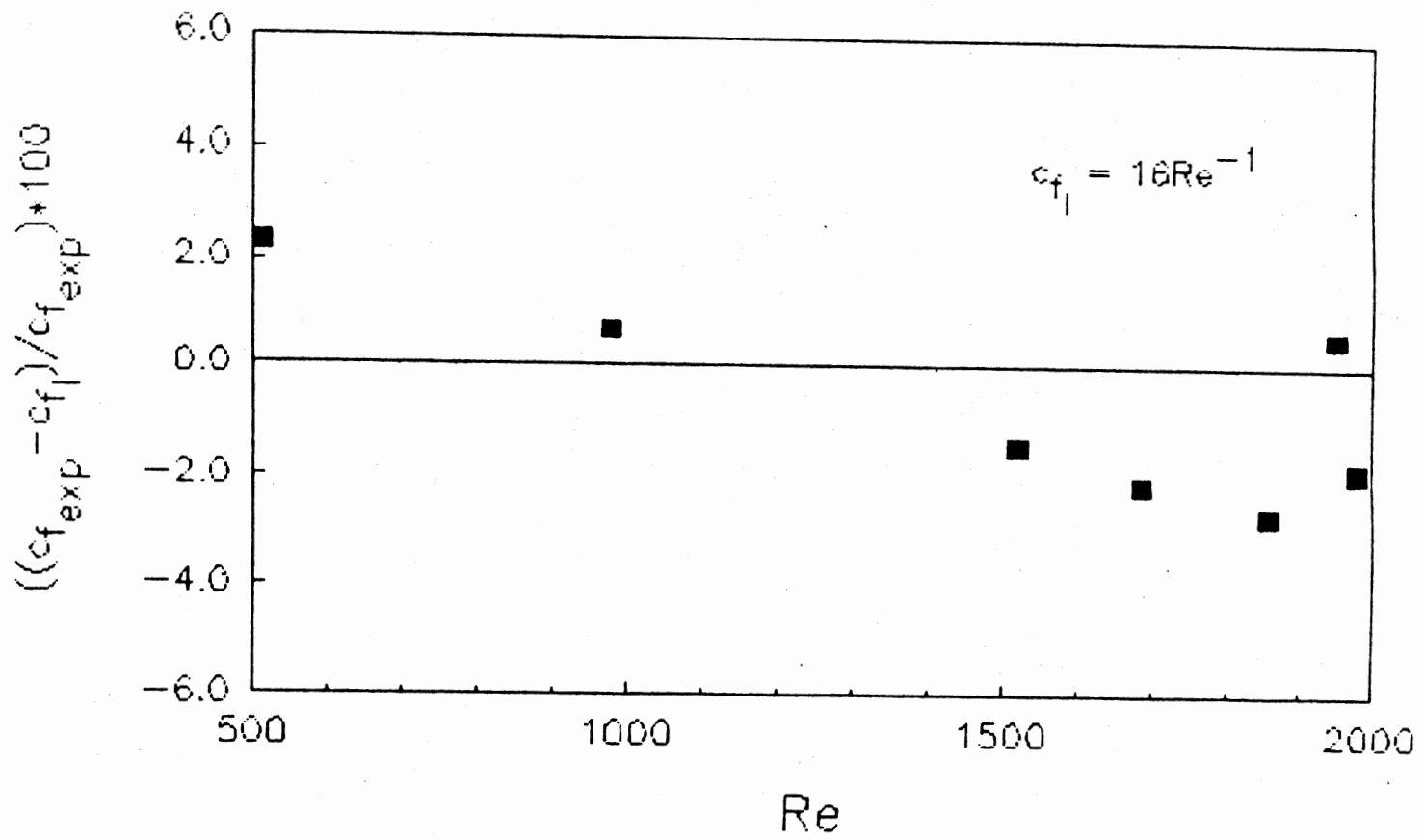
Figure 3.2   Percent Deviation from the Laminar Skin Friction Coefficient
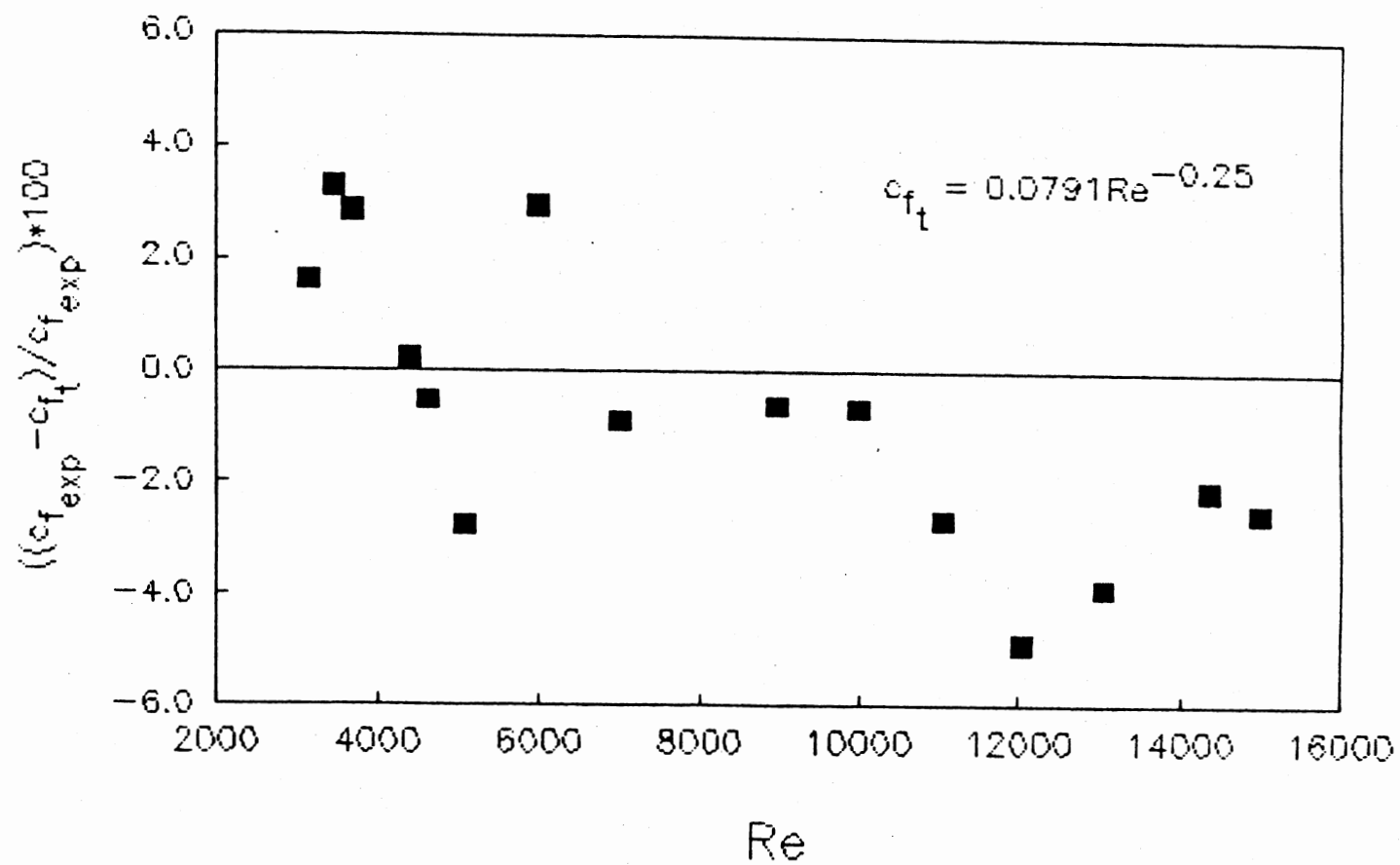
Figure 3.3 Percent Deviation from the Turbulent Skin Friction Coefficient

experimental data was not compared to them.

Transition Region

A magnified version of Figure 3.1 is included as Figure 3.4. This was done to isolate the transition region so its trends could be seen more clearly. Also included in Figure 3.4 are plots of transition region fully developed skin friction coefficient correlations by Churchill (1977), Hrycak & Andruskriw (1974), and Bhatti & Shah (1987). These correlations are listed in Table I. It can be seen that the experimental data shows the transition region occurring sooner (i.e. at a lower Reynolds number) and lasting for a smaller range of Reynolds numbers than the three correlations predict. This is where the effect of the highly disturbing square-edged entrance can be seen. The transition from laminar to transition flow was determined to occur at a Reynolds number of 2070. Transition flow developed into fully turbulent flow at a Reynolds number of 2840. Therefore, based solely on a fully developed skin friction coefficient the Blasius correlation was deemed accurate at Reynolds number as low as 2840 for this particular entrance in association with a smooth round tube. A rounded entrance or short bell mouth entrance was used in the development of the three established correlations. As predicted, the square-edged entrance produces a quicker transition and a higher degree of transition than a rounded entrance thus bringing about a fully developed turbulent flow at a lower
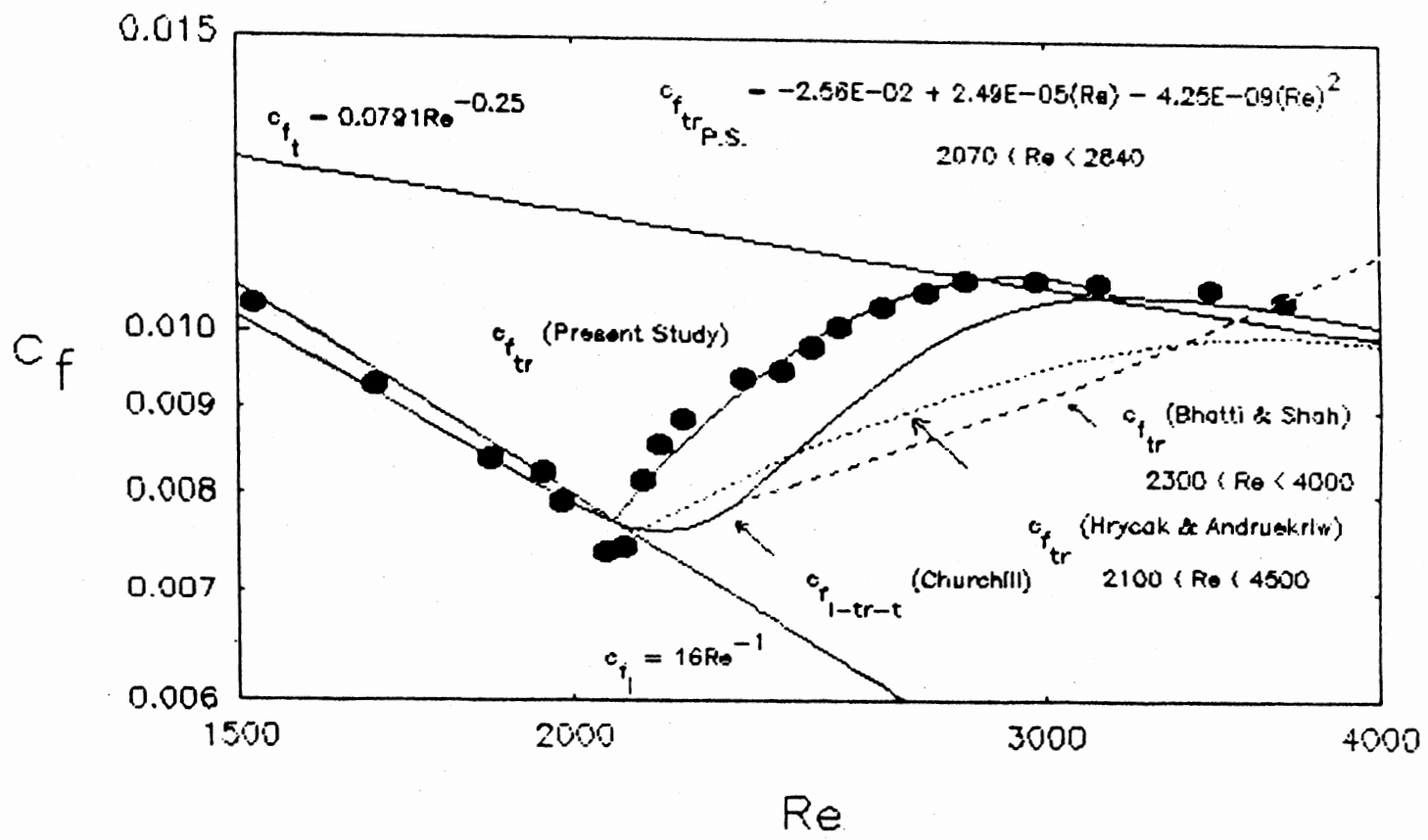
Figure 3.4 Moody Diagram of the Transition Region

Reynolds number. Since the data in the transition region was parabolic in nature the data was fit with a second order polynomial using the least squares method. The resulting correlation and its applicable range are listed below.

$$C_{ftr} = -2.56E\text{-}2 + 2.49E\text{-}5(Re) - 4.25E\text{-}9(Re)^2$$

$$2070 < Re < 2840$$

The percent deviation of the fourteen transition flow data points from the equation ranged from 4.08% to -4.91% with an average absolute percent deviation from the fit of 1.90%.

The second order polynomial was set equal to the laminar skin friction coefficient equation and a Reynolds number was solved for iteratively. The same was done with the Blasius correlation. This resulted in a range of Reynolds numbers, $2070 < Re < 2840$, where a fully developed skin friction coefficient could be predicted with the polynomial. The Reynolds numbers used in the curve fit ranged from 2055 to 3140. This was done to provide a more continuous set of data from which to fit a polynomial.

The parabolic nature of the fully developed skin friction coefficients in the transition region agrees well with the works of Ogawa & Kawamura (1987) and Senecal & Rothfus (1953). Also using a smooth round tube with a square-edged entrance Senecal and Rothfus determined the transition region to be $2100 < Re < 2800$. Their work is supported with pressure drop measurements and velocity profile measurements. Using a similar type entrance, Ogawa &

Kawamura reported the transition region to be

$2000 < Re < 3000$. Their work is supported with pressure drop

measurements only. Both of these works report data for the

fully developed region only, they report no data for the

entrance region. However, this study includes entrance

region information to augment that of the fully developed

region. It is important to note that air was used as a test

fluid in the works of Ogawa & Kawamura and Senecal & Rothfus.

By using liquids as a test fluid the data from this study

helps to confirm and improve upon the results of the

previously mentioned authors because of the different type of

fluid used.

A plot of the percent differences between the

experimental data and the derived correlation, Churchill's,

Hrycak & Andruskriw's, and Bhatti & Shah's correlations is

included as Figure 3.5. It should be noted that Hrycak &

Andruskriw's correlation is also a second order polynomial.

However, their correlation predicts transition flow to begin

at a Reynolds number of 2100 and end at a Reynolds number of

4500. Churchill's range of Reynolds numbers for the

transition region can visually be determined to be between

$Re = 2100$ and $Re = 3200$. This differs from the correlation

presented in this study because the disturbing nature of the

square-edged entrance used in this study causes transition to

start earlier and last for a smaller range of Reynolds

numbers. It is for this same reason that transition is

predicted earlier than it is for Churchill's correlation.
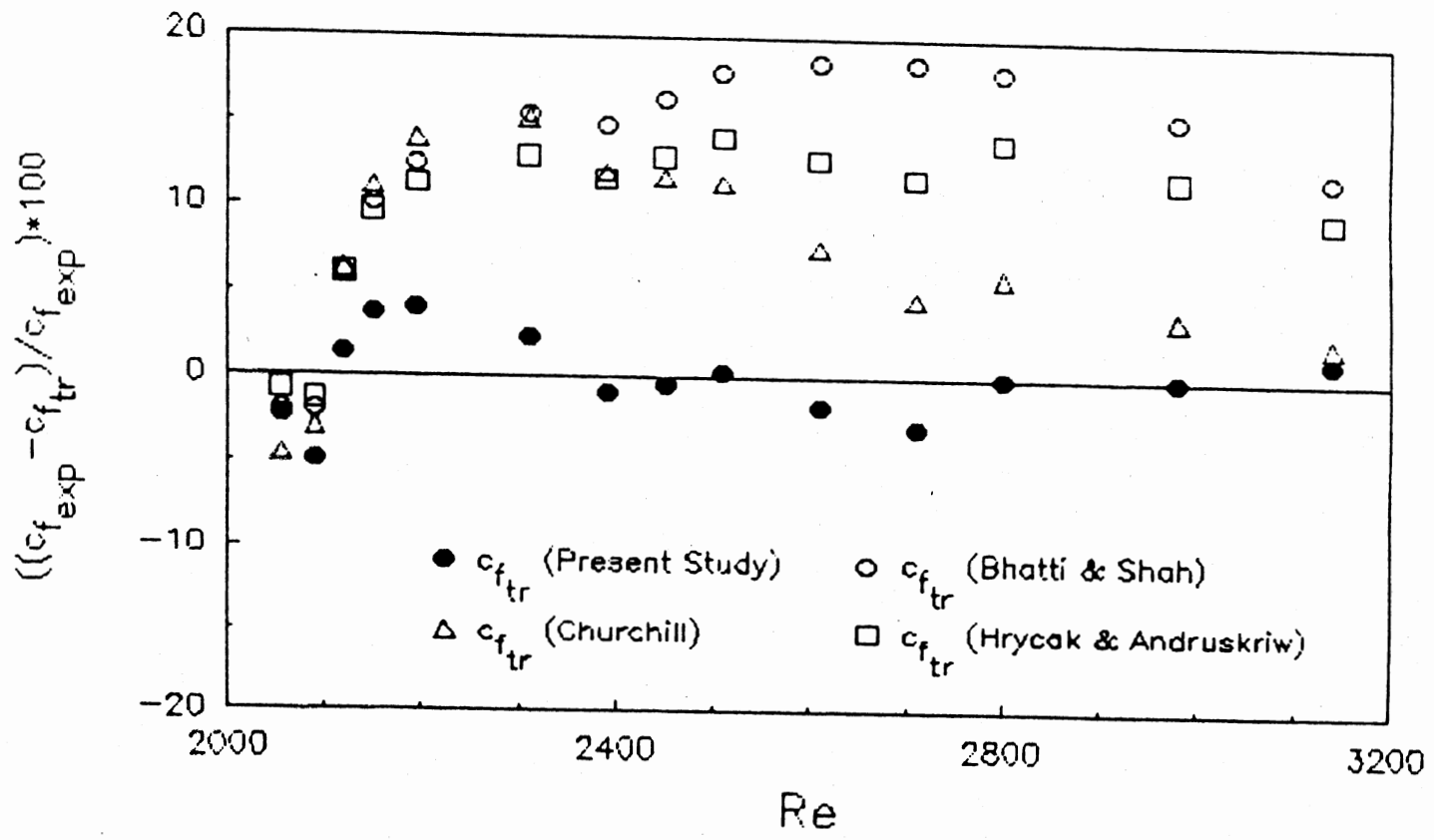
Figure 3.5   Percent Deviation from the Transition Skin Friction Coefficients

Churchill's correlation is not parabolic in nature because it is a model that continuously predicts fully developed friction factors in the laminar, transition, and turbulent flow regimes. Bhatti & Shah's correlation shows a different trend than does the data therefore its use is not recommended for circular tubes with a square-edged entrance. The correlation is not parabolic in nature and produces a sharp interface with turbulent line thus predicting a discontinuity from transition to turbulent flow. This study and others do not predict such discontinuities.

Length Required for a Fully Developed
Friction Factor

To further support the experimentally determined early onset of transition flow, two figures are included showing the apparent friction factors for laminar flow. Figure 3.6 displays apparent friction factor (f_{app}) versus the dimensionless axial location of the pressure taps (x/D) for five separate Reynolds numbers in the laminar range. It can be seen from this figure that as the Reynolds number increases the tube length required for the apparent friction factor to become constant decreases. For example; at a Reynolds number of 512 the friction factor becomes constant near 100 diameters, at a Reynolds number of 1860 the friction factor becomes constant near 60 diameters.

Figure 3.7 displays the same data in the form used by Langhaar (1942) with the apparent friction factor multiplied
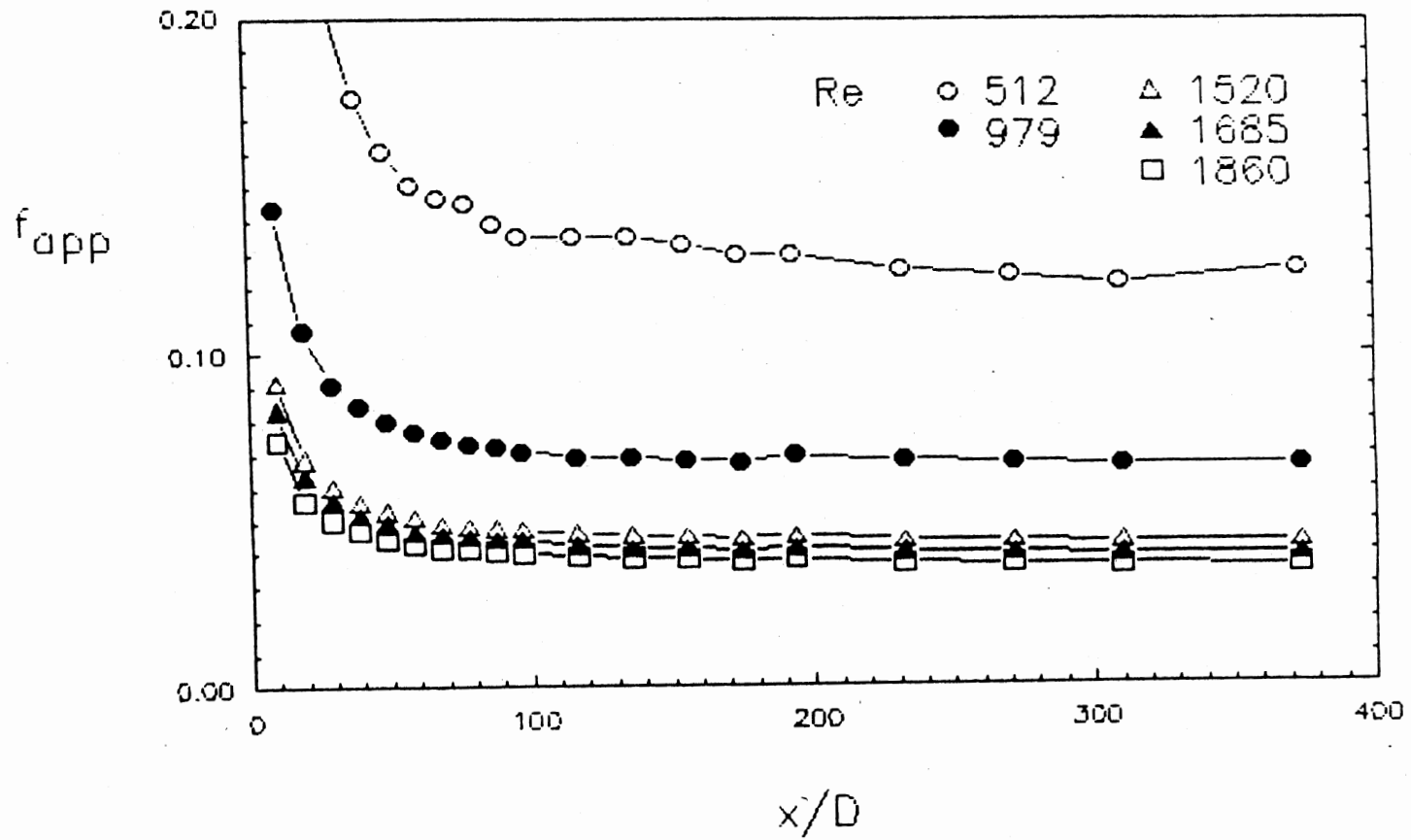
Figure 3.6   Laminar Flow Apparent Friction Factors
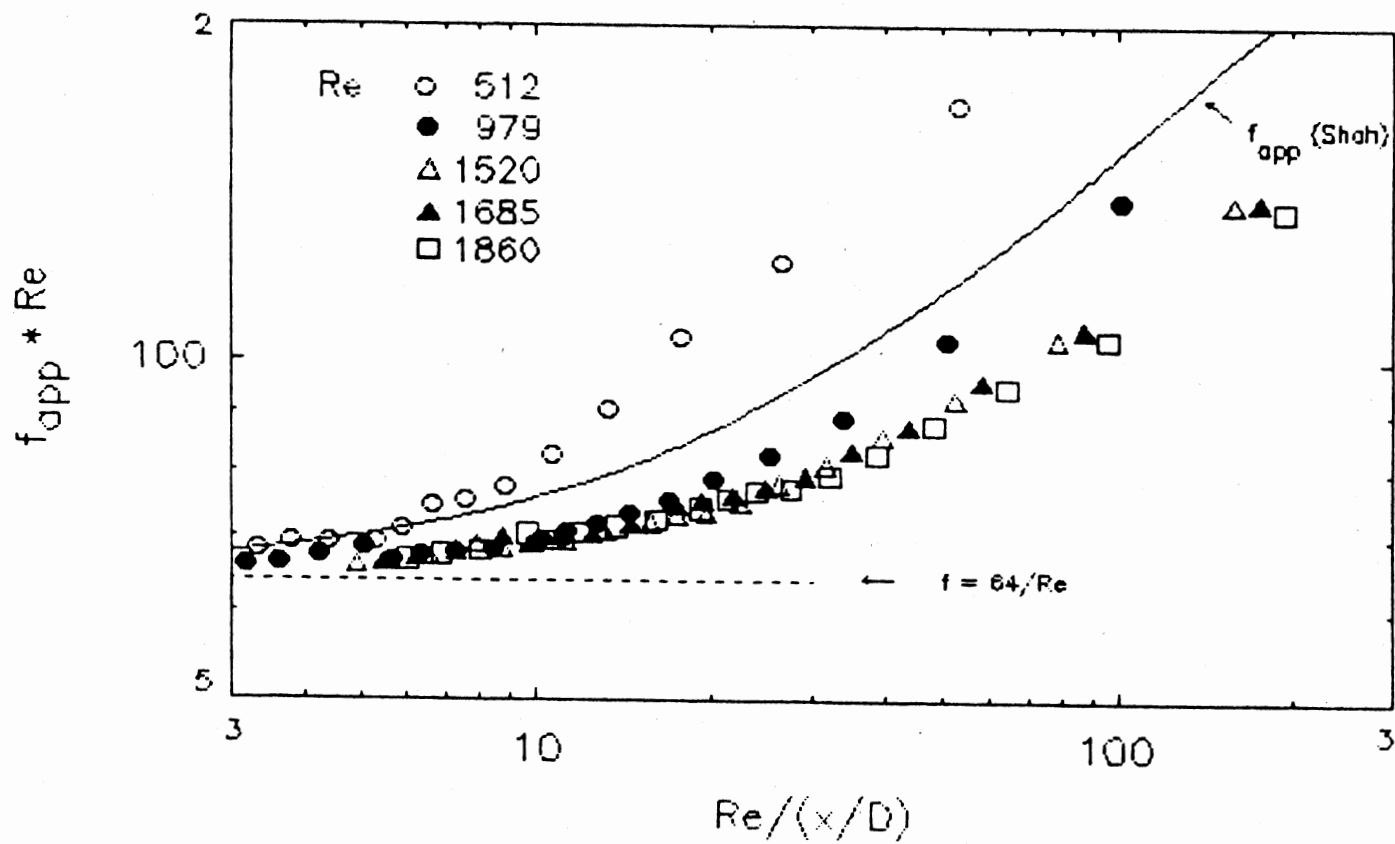
Figure 3.7 Laminar Friction Factors in the Entrance Region

by the Reynolds number versus the Reynolds number divided by
the dimensionless axial distance. Figure 3.7 also shows a
plot of the equation reported by Shah (1977), listed in Table
I, which is based on the theory of Langhaar. Langhaar's
theory for the hydrodynamic entry length for laminar flow in
smooth round tubes is based on a short bell-mouthed entrance
configuration as opposed to the square-edged entrance used
for this study. It can be seen that the data approaches the
line of f = 64/Re as expected. However, the data is shifted
to the right of the line predicted by Shah thus predicting a
shorter hydrodynamic entry length than Shah. It should be
noted that the term "hydrodynamic entrance length" refers to
the length required to fully develop the velocity profile.
However, in this study the hydrodynamic entrance length is
being compared to the tube length required for the friction
factor to become constant. It should also be noted that in
Langhaar's work the apparent friction factor line never
reaches the f = 64/Re line but the friction factor line does.
This is supported by the data because the data remains
slightly above the f = 64/Re line.

Although no velocity profile measurements were made and
the flow visualization study has yet to be completed it is
the author's intuition that states the square-edged entrance
used in this study causes the laminar boundary layer to grow
faster than a bell-mouthed entrance does thereby providing a
shorter length required for the friction factor to become
constant. By using Shah's correlation for a circular tube

with a square-edged entrance one could be in error by -34% to
57% in extreme cases, such as predicting apparent friction
factors near the inlet of a tube. The experimental data
begins to agree with Shah's correlation at Re/(x/D) values
less than 10.

It is assumed that since the inlet configuration has a
significant impact on the development of the laminar boundary
layer it must also have an impact on the range of Reynolds
numbers where transition flow occurs.

Figure 3.8, a figure similar to that of Figure 3.6 for
laminar flow, is included for fully turbulent Reynolds
numbers ranging from 5080 to 14970. From these plots of
turbulent apparent friction factors a correlation was
developed to predict the turbulent entrance length of
flows with Reynolds numbers ranging from 5000 to 15000. The
correlation that was developed is solely based on a fully
developed friction factor as opposed to being based on the
development of the velocity profile as was done by Latsko
(1921) and White (1986), reported by White. The data for the
turbulent entrance length correlation was obtained by
inspection of Figure 3.8 and visually determining the
pressure tap station where the apparent friction factor
became constant. Thus eleven data points were obtained and
curve fit was performed using the least squares method. This
data and the corresponding correlation appear on Figure 3.9.
The eleven data points used had an absolute average percent
deviation from fit of 9.56% and maximum of 14.9%. The
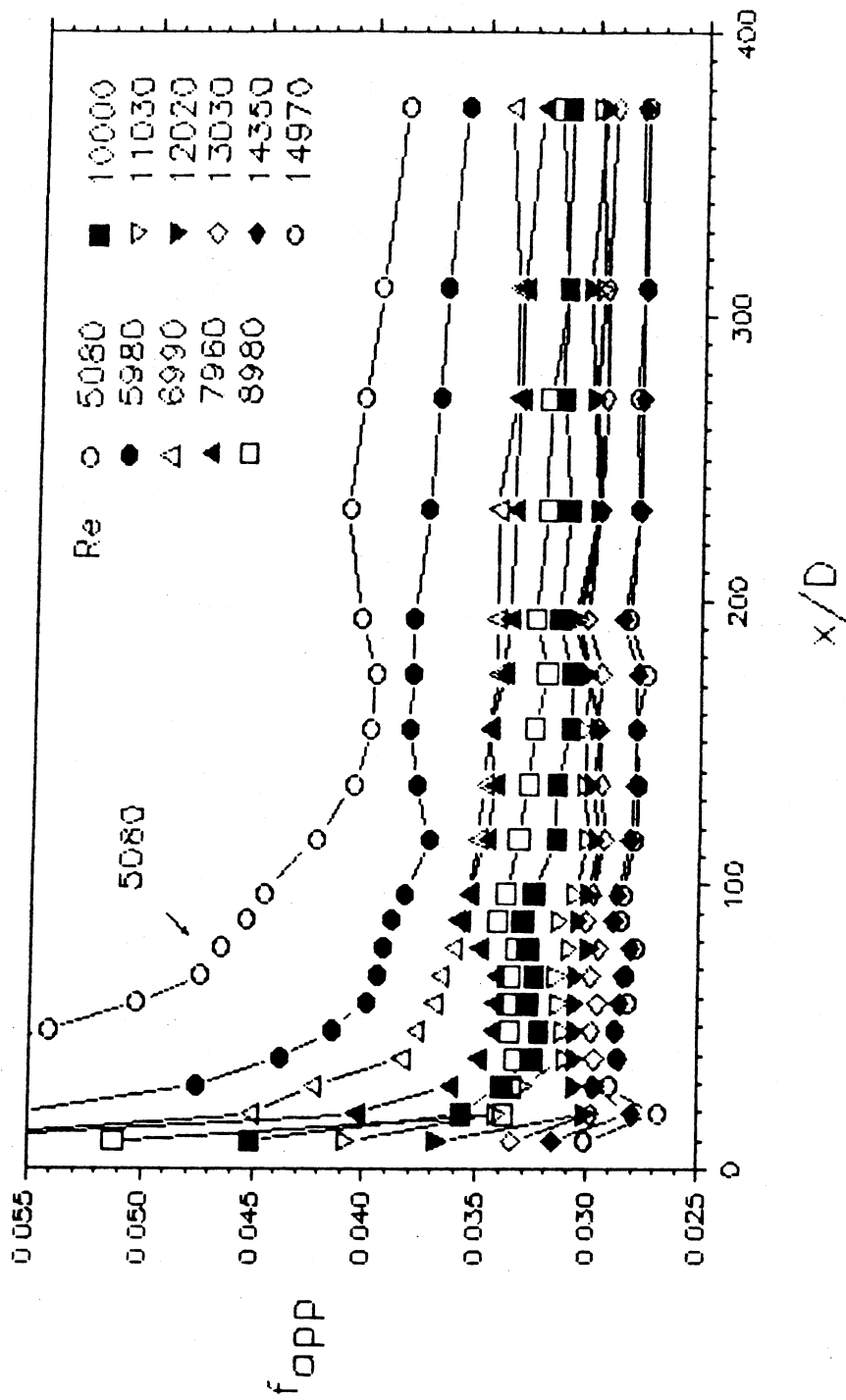
Figure 3.8   Turbulent Flow Apparent Friction Factors

$$(x/d) = 2.09*10^9 \, Re^{-1.66}$$

5000 < Re < 15000

Turbulent entrance length
is based on a fully developed friction factor
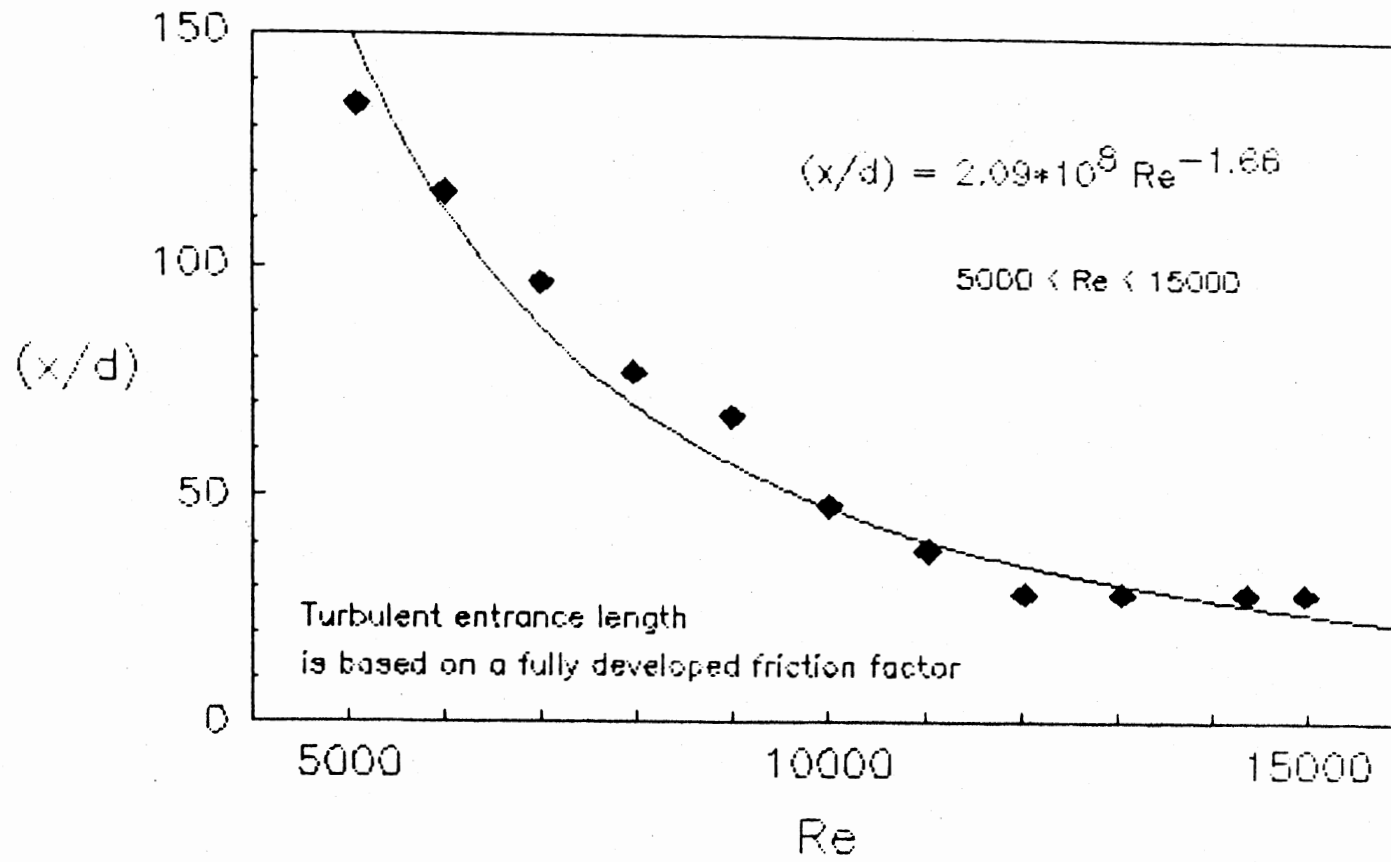
Figure 3.9 . Turbulent Entrance Length

maximum probable error in the data was 5.23%. It can be seen that the tube length required for the friction factor to become constant is inversely proportional to Reynolds number. This is exactly the opposite trend that correlations for the hydrodynamic entrance length predict. However, this is the same trend that appears on the plot of the laminar apparent friction factors, Figure 3.6. This is due to the fact that as the Reynolds number increases the skin friction between the fluid and the tube wall plays an increasing role in the pressure drop and begins to overshadow the role in the pressure drop played by the development of the velocity profile. The data shows that after Reynolds numbers greater than 20000 the flow can be considered fully developed turbulent flow at the entrance for the purpose of friction factor determinations. The author recommends the correlation stated in Figure 3.9 as a means of making an approximation as to how many diameters down a tube the fully developed friction factor correlations become valid for a smooth round tube with a square edged entrance. For example, at a Reynolds number of 10000 the friction factor would become constant near 50 diameters. A similar correlation was not developed for the laminar flow regime because the laminar flow data did not show as strong a trend as the turbulent data did.

CHAPTER IV

SUMMARY, CONCLUSIONS, AND RECOMMENDATIONS

In the previous chapter experimental data for pressure drop measurements in three fluid flow regimes (laminar, transition, and turbulent) in a smooth round tube with a square-edged entrance were presented. This chapter presents the accomplishments of the present study and gives recommendations for future study in this area.

Summary

A versatile experimental setup was constructed so that further research could be performed to determine the effects of different inlet configurations and the effects of a constant wall heat flux condition on the skin friction coefficient in the transition flow regime. The experimental setup also has the versatility to allow intermittency measurements to be made.

In order to cover the three flow regimes the range of Reynolds numbers covered was 512 to 14970. From this range of Reynolds numbers thirty three fully developed skin friction coefficients were obtained. These values are listed in Table II and displayed in Figure 3.1. The experimental data agreed quite well with the established correlations for fully developed laminar and turbulent skin friction

61

coefficients.

It was at a Reynolds number of 2070 where the fully
developed skin friction coefficients began to deviate from
the laminar line thus showing the onset of transition flow.
The critical Reynolds number is slightly lower than those
reported by other researchers because of the disturbing
nature of the square-edged entrance used in this study.
The fully developed skin friction coefficients in the
transition region increased in a parabolic nature until they
reached the turbulent line at a Reynolds number of 2840. The
reader is referred back to Figure 3.4 to review the trends of
the data reported compared with those of the correlation
reported in the literature. The second order polynomial used
to fit the data in the transition region and its applicable
range is

$$c_f = -2.56E-2 + 2.49E-5(Re) - 4.25E-9(Re)^2$$

$$2070 < Re < 2840$$

This correlation fits the data with an average absolute
percent deviation from fit of 1.90% and maximum absolute
percent deviation from fit of 4.91%. In performing the
uncertainty analysis, shown in Appendix C, it was determined
that the maximum probable error in the data was 5.23%.

It is the upper limit of this correlation which expands
the range of applicable Reynolds numbers where the Blasius
correlation is valid for a smooth round tube with a square-
edged entrance. The transition range reported in this study,

2070 < Re < 2840, compares well with those reported by Senecal & Rothfus (1953) for an identical inlet configuration and Ogawa & Kawamura (1987) for a similar inlet configuration. The transition skin friction coefficient correlation presented in this study is the first of its kind for a circular tube with square-edged entrance and helps to provide additional understanding about the long misunderstood region of transition flow. The correlation developed will be of most use to the heat exchanger industry since smooth round tubes with a square-edged entrance are commonly used in shell and tube heat exchangers.

Also of use to the heat exchanger industry is the correlation developed in this study to predict the turbulent entrance length for flow with Reynolds numbers ranging from 5000 to 15000.

$$x/D = 2.09E8(Re)^{-1.66}$$

This equation will aid designers in determining how far down a tube the Blasius friction factor becomes valid thus aiding in more accurate pumping power estimates.

For laminar flows in a smooth round tube with a square-edged entrance the tube length required for the friction factor to become constant is also inversely proportional to the Reynolds number. For example; at a Reynolds number of 512 the friction factor becomes constant near 100 diameters, at a Reynolds number of 1860 the friction factor becomes constant near 60 diameters.

Conclusions

The general conclusions drawn from this study may be summarized as follows:

1. The validity of the versatile experimental setup that was constructed was verified by the close agreement of the experimental data and the established skin friction coefficient correlations for fully developed laminar and turbulent flow. Therefore, the author is confident that pressure drop measurements made with different inlet configurations, under a constant wall heat flux condition, and involving intermittency measurements will provide valuable data.

2. A smooth round tube with a square-edged entrance produces a transition flow regime in the Reynolds number range of 2070 < Re < 2840. When plotted versus Reynolds number, the fully developed friction factors in the transition region are parabolic in nature.

3. The disturbing nature of the square-edged entrance is believed to cause the laminar boundary layer to grow faster thus resulting in shorter tube length required for the skin friction coefficient to become constant than predicted by the established correlation for a short bell-mouthed entrance in laminar flow.

4. The tube length required for the skin friction coefficient to become constant in the turbulent region with Reynolds numbers ranging from 5000 to 15000 is inversely proportional to the Reynolds number based solely on a fully developed skin friction coefficient. For Reynolds numbers greater than 20000 in smooth round tube with a square-edged entrance the flow can be considered fully developed at the entrance for the purpose of making pressure drop calculations.

Recommendations

The following recommendations made for future studies of this type are based on the observations made during this study.

1. Improvements can be made in performing pressure drop measurements of this type when a differential pressure transducers for liquids having differential pressures in the zero to fifty inwc range are developed. The differential pressure tranducers should be accurate to 0.01 inwc in order to make a significant improvement upon this study. The transducers would also probably have a much quicker response time than differential pressure gauges thereby allowing more data to be obtained.

2. It has been proven by other researchers that the Reynolds number range for transition flow is a

strong function of the inlet configuration. Other inlet configurations (such as bell-mouth and re-entrant inlet configurations) need to be studied to determine what effects they have on the transition region in smooth round tubes and the effects they have on the the tube length required to reach a fully developed friction factor.

3. Friction factors in the transition region under a constant wall heat flux condition need to be studied to determine what affect the induced heat flux has on inducing transition flow and to see if the transition region remains in the same range of Reynolds numbers for the same inlet. This type of study would also aid heat exchanger designers in predicting pumping power requirements. Studying transition flow friction factors for different inlets under a constant wall heat flux condition would further augment the work that has been done.

4. Introducing the concept of intermittency into the measurements already made and into future measurements could provide further validation of the transition range previously determined in this study. Intermittency measurements could also be introduced into the correlations developed in this study to determine if they compare well to those developed by Ogawa and Kawamura (1987).

REFERENCES

Benedict, R. P. (1984). *Fundamentals of Temperature, Pressure, and Flow Measurements.* John Wiley & Sons, New York.

Bhatti, M. S. and Shah, R. K. (1987). *Handbook of Single-Phase Convective Heat Transfer.* John Wiley & Sons, New York.

Bohn, D., Fischer, S., and Obermeir, E. (1984). Thermal Conductivity, Density, Viscosity, and Prandtl Numbers of Ethylene Glycol-Water Mixtures. *Ber. Bunsenges. Phys. Chem.* Vol. 88, pp. 739-742.

Churchill, S. W. (1977). Comprehensive Correlating Equations for Heat, Mass and Momentum Transfer in Fully Developed Flow in Smooth Tubes. *Ind. Eng. Chem. Fundam.* Vol. 16, pp. 109-116.

Hrycak, P. and Andrushkiw, R. (1974). Calculation of Critical Reynolds Number in Round Pipes and Infinite Channels and Heat Transfer in Transition Regions. *Heat Transfer.* Vol. II, pp. 183-187.

Langhaar, H. L. (1942). Steady Flow in the Transition Length of a Straight Tube. *Journal of Applied Mechanics.* Vol. 9, pp. A-55 – A-58.

Kline, S. J. and McClintock, F. A. (1953). Describing Uncertainties in Single Sample Experiments. *Mechanical Engineering.* Vol. 66, pp. 3-8.

Ogawa N. and Kawamura, H. (1987). Effects of Entrance Configuration on Pressure Loss and Heat Transfer of Transitional Gas Flow in a Circular Tube. *Heat Transfer Japanese Research.* Vol. 7, pp. 77-91.

Senecal, V. E. and Rothfus, R. R. (1953). Transition Flow of Fluids in Smooth Tubes. *Chemical Engineering Progress.* Vol. 10, pp. 533-538.

Shah, R. K. (1978). A Correlation for Laminar Hydrodynamic Entry Length Solutions for Circular and Noncircular Ducts. *Journal of Fluids Engineering.*

Shapiro, A. H. and Smith, R. D. (1957). Friction Coefficients in the Inlet Length of Smooth, Round Tubes. NACA. TN No. 1785, pp. 1-43.

Strickland, D. T. (1990). Heat Transfer Measurements in the Transition Region for a Circular Tube with a Square-Edged Entrance. MS Thesis, Oklahoma State University, Stillwater, Oklahoma.

White, F. M. (1986). <u>Fluid Mechanics.</u> McGraw Hill, New
     York.

APPENDIXES

APPENDIX A

DATA SOURCE

DATA SOURCE

The data for this study is available through

Dr. Afshin J. Ghajar
Asscociate Professor of Mechanical Engineering
School of Mechanical and Aerospace Engineering
Oklahoma State University
218 Engineering North
Stillwater, OK 74078
405-744-5900

APPENDIX B

SAMPLE CALCULATION

SAMPLE CALCULATION

The following sample calculation illustrates the procedure used to calculate a fully developed skin friction coefficient. The data used is that taken using distilled water at a Reynolds number of 6990.

After obtaining the average pressure drops using the procedure outlined in Chapter II, the average pressure drop from station fourteen is subtracted from the average pressure drop from station twenty. This procedure is repeated for stations fifteen through eighteen.

$$\Delta P_{20-14} = 2.0875 \text{ inwc}$$

$$\Delta P_{20-15} = 1.8750 \text{ inwc}$$

$$\Delta P_{20-16} = 1.4625 \text{ inwc}$$

$$\Delta P_{20-17} = 1.1125 \text{ inwc}$$

$$\Delta P_{20-18} = 0.7125 \text{ inwc}$$

To obtain a skin friction coefficient from the differential pressures equation (B.1) is used.

$$C_f = \frac{(\Delta P) \ (5.2) \ (D_i) \ (g_c)}{(1/2) \ (L) \ (V_{avg})^2 \ (\rho)} \tag{B.1}$$

5.2 is the necessary conversion factor to convert inwc to lbf/ft^2. The gravitational constant, g_c, is equal to 32.174 (lbm ft)/(lbf s^2). L is equal to the axial distance of the tube over which the pressure drop was measured. Equation (B.2) shows the differential pressure from stations fourteen to twenty and other pertinent data for the

particular Reynolds number entered into Equation (B.1).

$$C_{f20-14} = \frac{2.0875 \text{ inwc } \times 5.2 \text{ lbf/ft}^2/\text{inwc} \times 0.05175 \text{ ft} \times g_c}{2 \times 10.3021 \text{ ft} \times (1.29 \text{ ft/s})^2 \times 62.11 \text{ lbm/ft}^3}$$

(B.2)

$C_{f20-14} = 0.00849$

Similar calculations are performed to obtained the skin friction coefficients associated with the other pressure tap stations. The only variables that change in Equation (B.1) are the differential pressure, ΔP, and the tube length, L.

$C_{f20-15} = 0.00845$

$C_{f20-16} = 0.00840$

$C_{f20-17} = 0.00880$

$C_{f20-18} = 0.00905$

As stated in the section on data reduction, the high and low values are omitted and the remaining three averaged to obtain an average value of the skin friction coefficient for the particular Reynolds number.

$c_f = 0.00858$ at Re = 6990

Since this Reynolds number is in the fully turbulent flow regime it can be compared to the Blasius skin friction coefficient correlation.

$c_f = 0.0791 \text{ Re}^{-0.25}$ (B.3)

$= 0.0791 \text{ } (6990)^{-0.25}$

$c_f = 0.00865$

When comparing the two skin friction coefficients it can be seen that the experimental value deviates from the Blasius value by -0.9%.

APPENDIX C

UNCERTAINTY ANALYSIS

UNCERTAINTY ANALYSIS

The probable error in the experimental measurements of the skin friction coefficient is presented in this appendix. For a complete discussion of the theory of uncertainty analysis see Kline and McClintock (1953).

The skin friction coefficient is defined as

$$c_f = \tau_w/\tfrac{1}{2}\gamma_f U^2 = (D_i\Delta p/4L)/\tfrac{1}{2}\gamma_f U^2. \qquad (C.1)$$

In terms of the measured quantity it becomes

$$c_f = \frac{D_i\,\Delta p\,g}{2L\gamma\,[(mx + b)/(\pi/4)D_i{}^2]^2}. \qquad (C.2)$$

Here, the density of the fluid and the gravitational acceleration are assumed to be accurately known. The procedure for calculating the pressure drop depends upon whether the measurements were made using inches of water or inches of mercury. The term (mx + b) represents a volume flowrate and refers to the turbine meter calibration curves for the three different solutions that were used. This is explained further in the section on data reduction.

The uncertainty in the skin friction coefficient can be found from

$$\delta c_f = \{\ [(\partial c_f/\partial D_i)\delta D_i]^2 + [(\partial c_f/\partial G)\delta G]^2 + [(\partial c_f/\partial H)\delta H]^2$$
$$+ [(\partial c_f/\partial L)\delta L]^2 + [(\partial c_f/\partial F)\delta F]^2$$
$$+ [(\partial c_f/\partial T)\delta T]^2 \ \} \qquad (C.3)$$

The percentage uncertainty, which can be obtained with the

substitution of the partial derivatives of Equation (C.3) with respect to each variable into Equation (C.2) and division of its result by Equation (C.3), may be written as

$$(\delta c_i/c_i) \, (\%) = 100 * \{ \, (\delta D_i/D_i)^2 + (\delta G/G)^2 + (\delta H/H)^2 + $$
$$(\delta L/L)^2 + (-mF/(mF+b))^2 + (\delta T/T) \} \quad (C.4)$$

The uncertainty of each variable was estimated as follows:

δD_i : The uncertainty of the inside diameter of the test section was assumed to be 0.002".

δG : The accuracy of the differential pressure gauges was given by the manufacturer as + 3% full scale.

δH : The resolution of the mercury manometer was + .05". This value was taken as the uncertainty in H.

δL : The pressure tap interval was machined with an accuracy of + 0.002".

δF : The reading of the frequency from the turbine meters was influenced by the instantaneous change in flowrate. It was also affected by the calibration procedure. The probable error in F was assumed to be + 2.0 Hz.

δT : The accuracy of the reading of the fluid bulk temperature was assumed to be +0.5 F.

The following is a sample calculation of the uncertainty in calculating the skin friction coefficient.

$$\delta D_i/D_i = 0.002/0.621 = 0.00322$$
$$\delta G/G \quad = 0.03$$

$\delta H/H \quad = 0.05/1.47 = 0.0340$

$\delta L/L \quad = 0.002/6.000 = 0.000333$

$\delta F/F \quad = (0.0614*2)/(0.0648+0.0614*79) = 0.0250$

$\delta T/T \quad = 0.5/73.3 = 0.00682$

$(\delta c_f/c_f) \, (\%) = 100 * \{ (0.00322)^2 + (0.03)^2 + (0.0340)^2$

$$+ (0.000333)^2 + (0.025)^2$$

$$+ (0.00682)^2 \} \hspace{3cm} (C.5)$$

$(\delta c_f/c_f) \, (\%) = 5.23 \, \%$

Thus the maximum percent probable error in the skin friction coefficient is 5.23 %. It can be seen from Equation C.5 that the two greatest influences on the percent probable error are the uncertainty in the differential pressure gauges and the frequency counter reading.

APPENDIX D

COMPUTER PROGRAMS USED IN THE STUDY

ETH.BAS
FFC.BAS
GPMCALC.BAS

```
200  '
210  '   Jody R. Augustine
220  '   01-27-89
230  '
240  '   Thesis Program
250  '
260  '   Thermophysical Properties of Ethylene Glycol-Water Mixtures
270  '
280  '   Reference
290  '
300  '       D. Bohne, S. Fischer, and E. Obermeier:  "Thermal Conductivity,
310  '       Density, Viscosity, and Prandtl-Numbers of Ethylene Glycol-
320  '       Water Mixtures".  Ber. Bunsenges. Phys. Chem. 88, 742-744
330  '       (1984)
340  '
350  '   The program allows the user to input the mass concentration or
360  '   mass fraction of the ethylene glycol water-mixture along with
370  '   the bulk temperature of the mixture.  The wall temperature at
380  '   a specific thermocouple station may also be entered for the
390  '   purpose of obtaining a Grashof Number for natural convection
400  '   calculations.  The volumetric flow rate is also entered in order
410  '   to obtain an average tube velocity and a Reynolds Number.
420  '
430  '   The thermophysical property equations have a temperature range of
440  '   32 to 300 degrees Farenheit (0 to 150 degrees Celsius) at
450  '   atmospheric pressure.
460  '
470  '   The accuracy of the properties are as follows:
480  '
490  '       density         -+ 1%
500  '       thermal cond.   -+ 1%
510  '       abs. visc.      -+ 5%
520  '       Prandtl No.     -+ 5%
530  '
540  '   Variables ending with the letter (E) designate English units.
550  '
560  '
570  DEFDBL A-H,K-Z
580  RA = 1
590  CLS
600  '
610  INPUT "ENTER 1 FOR S.I. UNIT OUTPUT, RETURN FOR ENGLISH ";UN
620  '
630  INPUT "ENTER MASS CONCENTRATION (0 for water, 1 for pure eth. glyc.) ";X
640  IF X < 0 OR X > 1 THEN PRINT " MASS CONCENTRATION MUST BE BETWEEN ZERO AND
ONE " : GOTO 630
650  '
660  '
670  IF UN = 1 THEN 910
680  '
690  '
700  INPUT "ENTER BULK TEMPERATURE (F) ";T
```

```
710   IF T < 32 OR  T > 300 THEN PRINT " BULK TEMPERATURE MUST BE BETWEEN 32 AND
 300 DEGREES FARENHEIT" : GOTO 700
720   '
730   '
740   INPUT "ENTER WALL TEMPERATURE (F) ";TW
750   IF TW <= T OR TW > 500 THEN PRINT " WALL TEMPERATURE MUST BE GREATER THAN
THE BULK TEMPERATURE AND LESS THAN 500 F" : GOTO 740
760   '
770   '
780   INPUT "ENTER FLOWRATE (gpm) ";FL
790   IF FL < 0 OR FL > 20 THEN PRINT " FLOWRATE MUST BE BETWEEN 0 AND 20 gpm" :
 GOTO 780
800   '
810   '
820   INPUT "ENTER INSIDE TUBE DIAMETER (in.), default (.621 in.) ";DIAM
830   IF DIAM < 0 OR DIAM > 3 THEN PRINT " DIAMETER MUST BE BETWEEN 0 AND 3 INCH
ES" : GOTO 820
840   '
850   '
860   IF DIAM = 0 THEN DIAM = .621
870   DIAM = DIAM/12
880   '
890   IF UN = 0 THEN GOTO 1100
900   '
910   INPUT "ENTER BULK TEMPERATURE (C) ";T
920   IF T<0 OR T>150 THEN PRINT " BULK TEMPERATURE MUST BE BETWEEN 0 AND 150 DE
GREES CELSIUS" : GOTO 910
930   '
940   '
950   INPUT "ENTER WALL TEMPERATURE (C) ";TW
960   IF TW<T OR TW>300 THEN PRINT " WALL TEMPERATURE MUST BE GREATER THAN THE B
ULK TEMPERATURE AND LESS THAN 300 C" : GOTO 950
970   '
980   '
990   INPUT "ENTER FLOWRATE (m^3/min) ";FL
1000   IF FL<0 OR FL>1 THEN PRINT " FLOWRATE MUST BE GREATER THAN 0 AND LESS THA
N 1 m^3/min" : GOTO 990
1010   '
1020   '
1030   INPUT "ENTER THE TUBE INSIDE DIAMETER (mm), default (15.8 mm) ";DIAM
1040   IF DIAM<0 OR DIAM>100 THEN PRINT " TUBE I.D. MUST BE BETWEEN 0 AND 100 mm
 " : GOTO 1030
1050   '
1060   IF DIAM = 0 THEN DIAM = 15.8
1070   DIAM = DIAM * .0032808   ' converting mm to ft
1080   '
1090   FL = FL*264.17          ' converting m^3/min to gpm
1100   '
```

```
1110   PRINT
1120   PRINT
1130   IF RA = 0 THEN GOTO 1550
1140   '
1150   '
1160   DIM AD(3,3)                    'dimensioning arrays for curve fit coefficients
1170   DIM D(3,3)
1180   DIM AV(3,3)
1190   DIM V(2,3)
1200   DIM V2(3)
1210   DIM AP(3,3)
1220   DIM P(2,3)
1230   DIM P2(3)
1240   '
1250   AD(1,1) = 1.0004               'curve fit coefficients for density
1260   AD(1,2) = .17659
1270   AD(1,3) = -.049214
1280   AD(2,1) = -1.2379E-04
1290   AD(2,2) = -9.9189E-04
1300   AD(2,3) = 4.1024E-04
1310   AD(3,1) = -2.9837E-06
1320   AD(3,2) = 2.4614E-06
1330   AD(3,3) = -9.5278E-08
1340   '
1350   AV(1,1) = .55164               'curve fit coefficients for viscosity
1360   AV(1,2) = 2.6492
1370   AV(1,3) = .82935
1380   AV(2,1) = -.027633
1390   AV(2,2) = -.031496
1400   AV(2,3) = .0048136
1410   AV(3,1) = 6.0629E-17
1420   AV(3,2) = 2.2389E-15
1430   AV(3,3) = 5.879E-16
1440   '
1450   AP(1,1) = 2.5735               'curve fit coefficients for Prandtl-Numbers
1460   AP(1,2) = 3.0411
1470   AP(1,3) = .60237
1480   AP(2,1) = -.031169
1490   AP(2,2) = -.025424
1500   AP(2,3) = .0037454
1510   AP(3,1) = 1.1605E-16
1520   AP(3,2) = 2.5283E-15
1530   AP(3,3) = 2.3777E-16
1540   '
1550   IF UN = 1 THEN GOTO 1580
1560   T = (5/9)*(T-32)               'converting bulk temperature to degrees C
1570   '
1580   FOR I = 1 TO 3
1590       FOR J = 1 TO 3
1600           D(I,J) = AD(I,J)*X^(J-1)*T^(I-1)
```

```
1610        NEXT J
1620    NEXT I
1630    DENS =.D(1,1)+D(1,2)+D(1,3)+D(2,1)+D(2,2)+D(2,3)+D(3,1)+D(3,2)+D(3,3)
1640    '  units are g/cm^3
1650    '
1660    '
1670    PDRTA=    -1.2379E-04 -9.9189E-04*X +4.1024E-04*X*X
1680    PDRTB=    2*((-2.9837E-06*T +2.4614E-06*X*T -9.5278E-08*X*X*T))
1690    PDRT = PDRTA+PDRTB            ' part. deriv. of density wrpt temp.
1700    BETA = -(1/DENS)*(PDRT)       ' thermal expansion coefficient
1710    BETAF = (1/BETA)*1.8
1720    BETAE = 1/BETAF
1730    '
1740    FOR I = 1 TO 2
1750        FOR J = 1 TO 3
1760            V(I,J) = AV(I,J)*X^(J-1)*T^(I-1)
1770            V2(J) = AV(3,J)*X^(J-1)
1780        NEXT J
1790    NEXT I
1800    V3 = (V2(1)+V2(2)+V2(3))^.25*T*T
1810    VISC = V(1,1)+V(1,2)+V(1,3)+V(2,1)+V(2,2)+V(2,3) + V3
1820    ABVISC = EXP(VISC)
1830    '  units are mPa*s
1840    '
1850    '
1860    FOR I = 1 TO 2
1870        FOR J = 1 TO 3
1880            P(I,J) = AP(I,J)*X^(J-1)*T^(I-1)
1890            P2(J) = AP(3,J)*X^(J-1)
1900        NEXT J
1910    NEXT I
1920    P3 = (P2(1)+P2(2)+P2(3))^.25*T*T
1930    PRAN = P(1,1)+P(1,2)+P(1,3)+P(2,1)+P(2,2)+P(2,3) + P3
1940    PR = EXP(PRAN)
1950    '
1960    KH2O = .56276+.001874*T-.0000068*T*T
1970    KETH = .24511+.0001755*T-8.52E-07*T*T
1980    F = .6635-.3698*X-.000885*T
1990    K = (1-X)*KH2O + X*KETH - F*(KH2O-KETH)*(1-X)*X
2000    ' units are  W/m*K
2010    '
2020    '
2030    CP = PR*K/ABVISC         '  units are KJ/Kg*K
2040    '
2050    '
2060    DENSE = DENS*62.428               ' coverting from S.I. to English units
2070    ABVISCE = (ABVISC/1000)*.67197
2080    KE = K*.57818
2090    CPE = CP*.23901
2100    KINVISC = (ABVISC/DENS)
```

```
2110   KINVISCE = (ABVISCE/DENSE)
2120   '
2130   '
2140   T = T*1.8 + 32
2150   IF UN = 1 THEN TW = TW * 1.8 + 32
2160   GR = ((32.174*BETAE*DIAM^3*(TW-T))/(KINVISCE^2))/10000
2170   '
2180   VELE = (FL/7.48/((3.14159/4)*DIAM^2))/60
2190   VEL = VELE * .3048
2200   RE = VELE*(DIAM)/ KINVISCE/1000
2202   MFE = DENSE * ((3.141593/4)*DIAM^2) * VELE * 3600
2206   MF = DENS * 1000 * ((3.141593/4)*(DIAM*.3048)^2) * VEL
2210   '
2220   KINVISCE = KINVISCE * 3600 * 1000        ' scaling factors
2230   ABVISCE = ABVISCE * 3600
2240   BETA = BETA*10^3
2250   BETAE = BETAE * 10^3
2260   '
2270   TD = (K/(DENS*CP)) * 100       ' thermal diffusivity w/ scaling fact.
2280   TDE = (KE/(DENSE*CPE))*1000
2290   '
2300   IF UN = 1 THEN GOTO 2510
2310   '
2320   PRINT "Density  (lbm/ft^3)      = ";USING"###.##";DENSE
2330   PRINT "                                  Prandtl Number
 = ";USING"###.##";PR
2340   PRINT "Abs. Vis. (lbm/ft*hr)    = ";USING"###.##";ABVISCE
2350   PRINT "                                  Grashof Number * 10^-4
 = ";USING"###.##";GR
2360   PRINT "Kin. Vis. (ft^2/hr)*10^3 = ";USING"###.##";KINVISCE
2370   PRINT "                                  Velocity (ft/sec)
 = ";USING"###.##";VELE
2380   PRINT "Sp. Heat  (Btu/lbm*F)    = ";USING"###.###";CPE
2390   PRINT "                                  Reynolds No. * 10^-3
 = ";USING"###.###";RE
2400   PRINT "Th. Cond. (Btu/hr*ft*F)  = ";USING"###.###";KE
2407   PRINT "                                  Mass Flowrate (lbm/hr)
 = ";USING"####";MFE
2420   PRINT "Beta  (1/F)  * 10^3      = ";USING"###.###";BETAE
2430   PRINT
2440   PRINT "Th. Diff. (ft^2/hr) *10^3 = ";USING"###.##";TDE
2450   PRINT
2460   PRINT
2470   '
2480   IF UN = 0 THEN GOTO 2680
2490   '
2500   '
```

```
2510   PRINT "Density  (Kg/m^3) * 10^-3 = ";USING"###.###";DENS
2520   PRINT "                                Prandtl Number
   = ";USING"###.##";PR
2530   PRINT "Abs. Vis. (Kg/m*s)*10^3  = ";USING"###.##";ABVISC
2540   PRINT "                                Grashof Number * 10^-4
   = ";USING"###.##";GR
2550   PRINT "Kin. Vis. (m^2/s) * 10^6 = ";USING"###.##";KINVISC
2560   PRINT "                                Velocity (m/s)
   = ";USING"###.##";VEL
2570   PRINT "Sp. Heat (KJ/Kg*K)       = ";USING"###.##";CP
2580   PRINT "                                Reynolds No. * 10^-3
   = ";USING"###.##";RE
2590   PRINT "Th. Cond. (W/m*K)        = ";USING"###.###";K
2596   PRINT "                                Mass Flowrate (Kg/s)
   = ";USING"#.###";MF
2610   PRINT "Beta  (1/C)  * 10^3      = ";USING"###.###";BETA
2620   PRINT
2630   PRINT "Th. Diff. (m^2/s) * 10^8 = ";USING"###.##";TD
2640   PRINT
2650   PRINT
2660   '
2670   '
2680   INPUT "RUN AGAIN?  (Return for yes, any number for no) ";RA
2690   IF RA = 0 THEN GOTO 590
2700   '
2710   '
2720   END
```

```
2700   CLS
2710   '
2720   '       PROGRAM FFC.BAS
2730   '       JODY R. AUGUSTINE
2740   '       08-01-89
2750   '
2760   '       The program title "FFC" stands for Friction Factor
2770   '       Calculations.  This program reduces pressure drop data
2780   '       to friction factors for the specific experimental
2790   '       setup used in this study.  It is to be used in
2800   '       conjunction with the program ETH.BAS since it requires
2810   '       some of the values calculated in ETH.BAS.
2820   '
2830   OPEN "R21050.DAT" FOR OUTPUT AS #1
2840   IH$ = "INCHES H20"
2850   IM$ = "INCHES Hg"
2860   DEFINT S
2870   INPUT "ENTER THE LAST STATION READ IN INCHES OF H20 ";STH
2880   DIM FF(20)
2890   DIM DPH(20)
2900   DIM DPM(20)
2910   DIM LNTH(20)
2920   '
2930   '  defining the lengths of the tube with their
2940   '  respective pressure taps
2950   '
2960   LNTH(1) = .5
2970   LNTH(2) = 1
2980   LNTH(3) = 1.5
2990   LNTH(4) = 2
3000   LNTH(5) = 2.5
3010   LNTH(6) = 3
3020   LNTH(7) = 3.5
3030   LNTH(8) = 4
3040   LNTH(9) = 4.5
3050   LNTH(10) = 5
3060   LNTH(11) = 6
3070   LNTH(12) = 7
3080   LNTH(13) = 8
3090   LNTH(14) = 9
3100   LNTH(15) = 10
3110   LNTH(16) = 12
3120   LNTH(17) = 14
3130   LNTH(18) = 16
3140   LNTH(19) = 19.3021
3150   '
3160   IF STH < 1 THEN GOTO 3200
3170   FOR I = 1 TO STH
3180      INPUT " DELTA P = ";DPH(I):PRINT IH$:PRINT
3190   NEXT I
3200   K = STH+1
```

```
3210   FOR I = K TO 19
3220      INPUT " DELTA P = ";DPM(I):PRINT IM$:PRINT
3230   NEXT I
3235   '
3240   '  calculating the densities of differential pressure
3250   '  media
3260   '
3270   DENHG = 852.13 - .097111*TA
3280   DENH2O = 62.4
3290   '
3300   IF STH<2 THEN GOTO 3340
3310   FOR I = 1 TO STH
3320      FF(I) = DPH(I)*62.4*.621*2*32.174/(LNTH(I)*VELE*VELE*12*12*DENSE)
3330   NEXT I
3340   FOR I = K TO 19
3350      FF(I) = DPM(I)*DENHG*.621*2*32.174/(LNTH(I)*VELE*VELE*12*12*DENSE)
3360   NEXT I
3370   PRINT:PRINT
3380   LPRINT:LPRINT
3390   PRINT "  Re * 10^-3 = ";USING"##.###";RE
3400   LPRINT "  Re * 10^-3 = ";USING"##.###";RE
3410   PRINT "  DENHG = ";USING"###.#";DENHG
3420   LPRINT "  DENHG = ";USING"###.#";DENHG
3430   PRINT "  ";DATE$
3440   LPRINT "  ";DATE$
3450   PRINT #1," ";RE;" * 10^-3      ";DATE$
3460   PRINT:LPRINT
3470   PRINT "  ";STH;" IS THE LAST STATION READ IN IN. H2O"
3480   LPRINT "  ";STH;" IS THE LAST STATION READ IN IN. H2O"
3490   PRINT:LPRINT
3500   PRINT "    x/D       fapp     Av. dP"
3510   LPRINT "    x/D       fapp     Av. dP"
3520   PRINT:LPRINT
3530   FOR I = 1 TO STH
3540      PRINT USING "####.####";LNTH(I)/.05175,FF(I),DPH(I)
3550      LPRINT USING "####.####";LNTH(I)/.05175,FF(I),DPH(I)
3560      PRINT #1 , USING"####.#####";LNTH(I)/.05175,FF(I)
3570   NEXT I
3580   FOR I = K TO 19
3590      PRINT USING "####.####";LNTH(I)/.05175,FF(I),DPM(I)
3600      LPRINT USING "####.####";LNTH(I)/.05175,FF(I),DPM(I)
3610      PRINT #1 , USING "####.####";LNTH(I)/.05175,FF(I)
3620   NEXT I
3630   CLOSE #1
3640   LPRINT:LPRINT
3650   END
```

```
10 '                          PROGRAM GPMCALC.BAS
20 '                          DOUG STRICKAND
30 '              _           FEBUARY 28,1989
40 '
50 '    THIS PROGRAM WILL USE AN INPUT OF EITHER FREQUENCY OR FLOWRATE
60 '  AND FOR A SPECIFIED TURBINEMETER (LARGE OR SMALL) AND CALCULATE THE
70 '  UNSPECIFIED VALUE OVER THE RANGE OF GPM OR FREQUENCY AVAILABLE.
80 '
90 C=(4.28958E-03+4.30351E-03+4.28176E-03)/3
100 C1=(6.952761E-02+.0692793+.068818)/3
110 K=-(.021509+.026951+.017774)/3
120 K1=-(.13566+.084517+.033494)/3
130 CLS
140 PRINT"  YOU CAN EITHER CALCULATE FLOWRATE FROM FREQ. OR VICE VERSA"
150 PRINT
160 INPUT"  ENTER  '1'  TO CALCULATE GPM, ENTER  '2'  TO CALCULATE FREQ.";W
170 IF W=1 THEN CLS: GOTO 540
180 CLS
190 PRINT" WHICH FLOWMETER DO YOU WANT FREQUENCY DATA FOR?"
200 PRINT
210 INPUT" ENTER '1' FOR SMALL METER, ENTER '2' FOR LARGE METER";V
220 IF V=1 THEN CLS: GOTO 390
230 CLS
240 INPUT" WHAT IS THE FLOWRATE FOR THE LARGE METER (GPM)";GPM
250 HF=((GPM-K1)/C1)
260 IF GPM<3.72 GOTO 350
270 IF GPM>10.25 GOTO 350
280 CLS
290 PRINT USING"           FREQUENCY = ###.#### HERTZ";HF
300 PRINT
310 PRINT USING"        FOR A FLOWRATE OF ##.#### GPM";GPM
320 PRINT
330 GOTO 950
340 CLS
350 PRINT
360 PRINT" THE FLOWRATE INPUT IS NOT AVAILABLE FOR THE LARGE METER."
370 PRINT
380 GOTO 900
390 INPUT" WHAT IS THE FLOWRATE FOR THE SMALL METER";GPM
400 SF=((GPM-K)/C)
410 IF GPM<.56 GOTO 500
420 IF GPM>4.61 GOTO 500
430 CLS
440 PRINT USING"           FREQUENCY = ####.#### HERTZ";SF
450 PRINT
460 PRINT USING"         FOR A FLOWRATE OF #.#### GPM";GPM
470 PRINT
480 GOTO 950
490 CLS
500 PRINT
```

```
510 PRINT" THE FLOWRATE INPUT IS NOT AVAILABLE FOR THE SMALL METER"
520 PRINT
530 GOTO 900
540 PRINT"  WHICH FLOWMETER DO YOU REQUIRE GPM DATA FOR? "
550 PRINT
560 INPUT"  ENTER '1' FOR SMALL METER, ENTER '2' FOR LARGE METER";A
570 PRINT
580 IF A=1 THEN CLS: GOTO 770
590 CLS
600 INPUT"  ENTER THE FREQUENCY FOR THE LARGE TURBINEMETER";LF
610 IF LF<55 GOTO 710
620 IF LF>155 GOTO 710
630 GPM=C1*LF+K1
640 CLS
650 PRINT
660 PRINT USING"            FLOWRATE= ##.#### GPM";GPM
670 PRINT
680 PRINT USING" FOR A FREQUENCY OF  ###.### HERTZ";LF
690 GOTO 930
700 CLS
710 PRINT" THE FREQUENCY INPUT IS NOT IN THE AVAILABLE LARGE METER RANGE"
720 PRINT
730 INPUT" DO YOU WISH TO TRY AGAIN (YES=1 NO=2)";B
740 IF B=2 THEN CLS: GOTO 970
750 GOTO 130
760 PRINT
770 INPUT"  ENTER THE FREQUENCY FOR THE SMALL TURBINEMETER IN Hz";SF
780 IF SF<135 GOTO 870
790 IF SF>1080 GOTO 870
800 GPM=C*SF+K
810 CLS
820 PRINT
830 PRINT USING"              FLOWRATE =##.#### GPM";GPM
840 PRINT
850 PRINT USING"    FOR A FREQUENCY OF  ####.#### HERTZ";SF
860 GOTO 930
870 CLS
880 PRINT" THE FREQUENCY INPUT IS NOT AVAILABLE FOR THE SMALL METER"
890 PRINT
900 INPUT" DOU YOU WISH TO TRY AGAIN  (YES=1 NO=2)";B1
910 IF B1=2 THEN CLS: GOTO 970
920 GOTO 130
930 PRINT
940 PRINT
950 INPUT" TO RUN THE PROGRAM AGAIN, ENTER '1', TO STOP ENTER '2'";Z
960 IF Z=1 GOTO 130
970 END
```

APPENDIX E

THERMOPHYSICAL PROPERTIES OF WATER AND ETHYLENE GLYCOL SOLUTIONS

Physical Properties of Ethylene Glycol-Water Mixtures

The correlations for the physical properties were reported in ref. (1).

Density

$$\rho = \sum_{i=1}^{3} \sum_{j=1}^{3} A_{ij} x^{(j-1)} T^{(i-1)}$$

where

Values of A_{ij}

	j=1	j=2	j=3
i=1	1.0004	0.17659	-0.049214
i=2	-1.2379×10^{-4}	-9.9189×10^{-4}	4.1024×10^{-4}
i=3	-2.9837×10^{-6}	2.4614×10^{-6}	-9.5278×10^{-8}

ρ = density, g/cm^3

x = mass fraction of ethylene-glycol

T = temperature, °C

This equation has an accuracy within $\pm 0.25\%$. It is applied over the temperature range of 0 to 150°C.

Comparison of density correlation with other sources

Pure Water	-0.1%	ref. (4)
	0% to 0.1%	ref. (7)
Pure EG	-1.0% to -0.2%	ref. (6)
30% EG	-0.2% to 0.3%	ref. (2)
50% EG	-0.2% to 0%	ref. (2)
70% EG	-0.2% to 0.1%	ref. (2)

Viscosity

$$\ell n\mu = \sum_{i=1}^{2} \sum_{j=1}^{3} A_{ij} x^{(j-1)} T^{(i-1)} + \{\sum_{j=1}^{3} A_{3j} x^{(j-1)}\}^{\frac{1}{4}} T^2$$

where

Values of A_{ij}

	j=1	j=2	j=3
i=1	0.5614	2.6492	0.82935
i=2	-2.7633×10^{-2}	-3.1496×10^{-2}	4.8136×10^{-3}
i=3	6.0629×10^{-17}	2.2389×10^{-15}	5.8790×10^{-16}

μ = viscosity, mPa-s

x = mass fraction of ethylene glycol

T = temperature, °C

This equation has an accuracy within ±0.25%. It is applied over the temperature range of 0 to 150°C.

Comparison of viscosity correlation with other sources

Pure Water	-7% to 3%	ref. (4)
	-12% to 10%	ref. (7)
Pure EG	-3.7% to 0.3%	ref. (6)
30% EG	-10% to 5%	ref. (2)
50% EG	-9% to 7%	ref. (2)
70% EG	-4% to 0%	ref. (2)

Thermal Conductivity

$$K_W = 0.56276 + 1.874\times10^{-3}T - 6.8\times10^{-6}T^2$$

$$K_{EG} = 0.24511 + 1.755\times10^{-4}T - 8.52\times10^{-7}T^2$$

$$K_F = 0.6635 - 0.3698x - 8.85\times10^{-4}T$$

$$K_M = (1-x)K_W + xK_{EG} - K_F(K_W - K_{EG})(1-x)x$$

where

K_W = thermal conductivity of pure water, W/m-K

K_{EG} = thermal conductivity of pure ethylene glycol, W/m-K

K_F = Filippov's constant

K_M = thermal conductivity of ethelyne glycol-water mixture, W/m-K

x = mass fraction of ethylene glycol

T = temperature, °C

The equation has an accuracy within ±1%. It is applied over the temperature range of 0 to 150°C.

Comparison of thermal conductivity correlation with other sources

Pure Water	-0.3% to 0.3%	ref. (4)
	-0.7% to 0.1%	ref. (7)
Pure EG	-4.1% to -3.1%	ref. (6)
30% EG	-4.6% to 0.3%	ref. (2)
50% EG	-10% to 2%	ref. (2)
70% EG	-11% to 6%	ref. (2)

Prandtl Number

$$\ln Pr = \sum_{i=1}^{2} \sum_{j=1}^{3} A_{ij} \, x^{(j-1)} T^{(i-1)} + \{ \sum_{j=1}^{3} A_{3j} \, x^{(j-1)} \}^{\frac{1}{4}} T^2$$

where

Values of A_{ij}

	j=1	j=2	j=3
i=1	2.5735	3.0411	0.60237
i=2	-3.1169×10^2	-2.5424×10^{-2}	3.7454×10^{-3}
i=3	1.1605×10^{-16}	2.5283×10^{-15}	2.3777×10^{-17}

Pr = Prandtl number, $\mu C_p / K$

x = mass fraction of ethylene glycol

T = temperature, °C

This equation has an accuracy within ±5%. It is applied over the temperature range of 0 to 150°C.

Comparison of Prandtl Number correlation with other sources

Pure Water	− 5% to 2%	ref. (4)
	−15% to 10%	ref. (7)
Pure EG	− 5% to 4%	ref. (6)

Coefficient of Thermal Expansion

$$\beta = -(1/\rho) \{-1.2379 \times 10^{-4} - 9.9189 \times 10^{-4}\, x + 4.1024 \times 10^{-4}\, x^2$$
$$+2(-2.9837 \times 10^{-6}\, T + 2.4614 \times 10^{-6}\, x\, T - 9.5278 \times 10^{-8}\, x^2 T)\}$$

where

β = coefficient of thermal expansion, 1/°C

ρ = density, g/cm^3

x = mass fraction of ethylene glycol

T = temperature, °C

This equation was derived from the relation $\beta = (1/\rho)\, (\partial\rho/\partial T)_p$, with the use of the density correlation listed previously. It is applied over the temperature range of 0 to 150°C.

Comparison of β correlation with other sources

Pure Water	−18% to −3%	ref. (3)
Pure EG	5% to 8%	ref. (5)

Comparison of secondary properties (properties that were calculated from the listed correlations) with other sources.

Kinematic Viscosity

ν = Kinematic viscosity, m^2/s

$\nu = \mu/\rho$

Pure Water	-7% to 3%	ref. (4)
Pure EG	-3% to 1%	ref. (6)

Specific Heat

C_p = specific heat, J/kg-K

$C_p = PrK/\mu$

Pure Water	0.3% to 1.2%	ref. (4)
	-0.7% to 0.6%	ref. (7)
Pure EG	-4%	ref. (6)
30% EG	-5% to -3%	ref. (2)
50% EG	-2% to 2%	ref. (2)
70% EG	-1% to 0%	ref. (2)

Thermal Diffusivity

α = thermal diffusivity, m^2/s

$\alpha = K/\rho C_p$

Pure EG	1% to 1.5%	ref. (6)

References

1. Bohn, D., Fischer, S., and Obermeir, E. "Thermal Conductivity, Density, Viscosity and Prandtl Numbers of Ethylene Glycol-Water Mixtures" Ber. Bunsenges. Phys. Chem. Vol. 88, pp. 739-742 (1984).

2. Glycols, Union Carbide Chemicals Co., New York (1985).

3. Heat Exchanger Design Handbook, Hemisphere Publishing Corp. (1983).

4. Kays, W.M., and Crawford, M.E., Convective Heat and Mass Transfer, McGraw Hill, New York (1980).

5. Moshfeghian, M., Fluid Flow and Heat Transfer in U-Tube Bends, Ph.D. Thesis, Oklahoma State University, Stillwater, OK (1978).

6. White, Frank M., Heat and Mass Transfer, Addison Wesley, New York (1988).

7. Zografos, A.I., Martin, W.A., and Sunderland, J.E., "Equations of Properties as a Function of Temperature for Seven Fluids", Computer Methods in Applied Mechanics and Engineering, v. 61, pp. 177-187 (1987).

VITA

Jody R. Augustine

Candidate for the Degree of

Master of Science

Thesis: PRESSURE DROP MEASUREMENTS IN THE TRANSITION REGION
FOR A CIRCULAR TUBE WITH A SQUARE-EDGED ENTRANCE

Major Field: Mechanical Engineering

Biographical:

Personal Data: Born in McKinney, Texas, June 3, 1965,
the son of Roy C. and Connie Augustine.

Education: Graduated from Holy Savior Menard Central
High School, Alexandria, Louisiana, in May, 1983;
received Bachelor of Science Degree in Mechanical
Engineering from The University of Southwestern
Louisiana in May, 1988; completed requirements
for the Master of Science Degree at Oklahoma State
University in May, 1990.

Professional Experience: Teaching Assistant, Department
of Mechanical & Aerospace Engineering, Oklahoma
State University, August, 1988, to December, 1989.
Research Assistant, Department of Mechanical &
Aerospace Engineering, Oklahoma State University,
January, 1989, to December, 1989.